INORGANIC CHEMISTRY FRONTIERS

REVIEW

View Article Online
View Journal | View Issue

Cite this: *Inorg. Chem. Front.*, 2024, **11**, 5833

Recent advances in the mechanism and catalyst design in the research of aprotic, photo-assisted, and solid-state Li–CO_2 batteries

Haixia Chen,[a] Xijuan Li,[a] Hairong Xue,*[b] Lulu Jia,*[d] Yunyun Xu,[a] Yinglei Tao,[a] Yige Yan,[e] Xiaoli Fan,*[c] Jianping He [a] and Tao Wang *[a]

Carbon dioxide (CO_2), resulting from the combustion of fossil fuels, is widely recognized as one of the main contributors to global warming. However, the existing carbon capture methods lack stability and cost-effectiveness. In order to tackle this issue, lithium-carbon dioxide batteries (LCBs) have emerged as a promising solution due to their high energy density and environmentally friendly nature. Nevertheless, the development of LCBs is still in its early stages, facing challenges such as low catalyst efficiency, electrolyte system instability, and an unclear mechanism. This review focuses on the reaction mechanism and cathodic catalysts of various types of LCBs, which include aprotic LCBs, photo-assisted LCBs, and all-solid-state LCBs. Lastly, the review paper summarizes the current problems and challenges associated with LCBs, providing suggestions and solutions to further advance the development and research of the LCB system.

Received 23rd June 2024,
Accepted 30th July 2024

DOI: 10.1039/d4qi01570c

rsc.li/frontiers-inorganic

1. Introduction

With the ongoing utilization of fossil fuel energy sources, a considerable amount of CO_2-based greenhouse gases has been emitted into the atmosphere, resulting in an energy crisis and global warming.[1,2] Achieving the goal of "carbon neutrality" poses a significant challenge, necessitating the development of energy storage and clean energy systems.[3–5] LCBs have garnered increasing attention from researchers due to their potential to effectively utilize CO_2 as a reactive substance, showing excellent theoretical specific capacity and energy density.[6,7] LCBs have higher theoretical energy density compared to various types of batteries such as Na-ion batteries,[8] Li-ion batteries,[9] *etc.*, which gives advantages for applications in fields with high energy density requirements. Compared with other metal–air batteries, such as Zn–air batteries[10] and Mg–air batteries,[11] LCBs are able to utilize CO_2 as the active substance, which reduces the weight of the battery and provides more possibilities for the design of the spatial structure of the device. LCBs are well-suited for exploration or submarine missions on CO_2-filled Mars environments,[12] serving as a valuable medium for energy utilization and storage.

However, several issues contribute to the failure of LCBs, such as carbon deposition on the cathode surface, electrolyte decomposition, electrolyte short-circuiting caused by lithium dendrites, sluggish CO_2 reduction reaction and CO_2 oxidation reaction (CRR and CER) kinetics affecting the battery efficiency, and repeated formation of Li_2CO_3 leading to structural instability and a reduced lifespan. These problems present significant challenges for the application and advancement of LCBs. Therefore, a comprehensive understanding of the mechanisms involved during the charging and discharging of LCBs, as well as the role of cathode catalysts in enhancing battery reaction kinetics, is of paramount importance for battery research and development. Mu *et al.* provided a comprehensive summary of the reaction mechanism, catalysts, and electrolyte working mode in LCBs.[12] Furthermore, while improving polarization through electrocatalysts is often limited, the development of photocatalysts offers an effective strategy to address this issue.[13,14] Additionally, the safety concerns arising from electrolyte leakage and volatilization in liquid systems pose limitations in the application of LCBs,

[a]*Centre for Hydrogenergy, College of Materials Science and Technology, Nanjing University of Aeronautics and Astronautics, Nanjing 210016, P. R. China. E-mail: wangtao0729@nuaa.edu.cn*
[b]*Zhongyuan Critical Metals Laboratory, School of Materials Science and Engineering, Zhengzhou University, Zhengzhou, Henan 450001, P. R. China. E-mail: xuehairong@zzu.edu.cn*
[c]*School of Materials Science and Engineering, Nanjing Institute of Technology, Nanjing 211167, P.R. China. E-mail: fanxl@njit.edu.cn*
[d]*Graduate School of Advanced Science and Engineering, Waseda University, 2-8-26 Nishiwaseda, Shinjuku, Tokyo 169-0051, Japan. E-mail: jia.lulu@akane.waseda.jp*
[e]*Institut de recherches sur la catalyse et l'environnement de Lyon (IRCELYON), UMR5256, PRETTRE building, 2 avenue Albert Einstein, Villeurbanne cedex 69626, France*

making the development of all-solid-state batteries a viable solution.[15–17]

In recent years, LCBs have made significant advancements, including continuous innovation in catalyst materials, further understanding of reaction mechanisms, improvement in the cycle life and battery efficiency, and potential commercial deployment. Ongoing research and technological progress are driving LCBs closer to practical feasibility for energy storage and conversion applications, while also influencing the development of photo-assisted LCBs and all-solid-state LCBs to some extent. LCBs began to come into the view of researchers from 2011 when Takechi *et al.* proposed Li–CO_2/O_2 as a prototype for LCBs.[7] Recently, the number of studies on LCBs has grown steadily, covering a wide range of topics from electrode material design to reaction mechanisms. Previous studies have summarized the role of electrocatalysts in regulating the electrochemical performance of LCBs in liquid systems, as well as the reaction mechanisms in different systems.[18,19] However, limited research has been conducted on the latest advancements in photo-assisted LCBs and all-solid-state systems. In this review, we provide a comprehensive overview of the latest research on the reaction mechanism and design of cathode catalysts for aprotic/photo-assisted/solid-state LCBs (Fig. 1). Furthermore, we introduce emerging photo-assisted LCBs and all-solid-state LCBs, delving deep into the impact of light fields and the role of solid-state electrolytes on LCBs. This review highlights the challenges faced by conventional LCBs and nascent photo-assisted/all-solid-state LCBs, while proposing solutions and suggestions to facilitate the further development of LCBs.

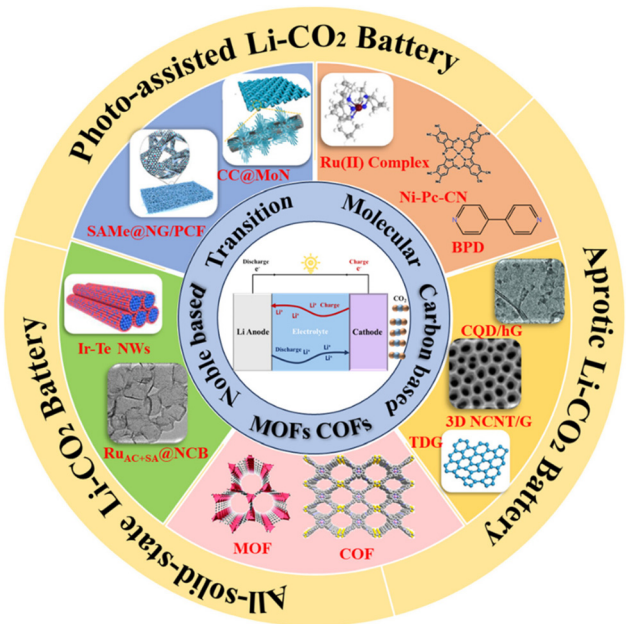

Fig. 1 Schematic elaboration of catalysts for the aprotic/photo-assisted/solid-state Li–CO_2 battery.

2. Mechanism of reversible LCBs

The mechanism of the electrochemical reaction process of LCBs is complex and involves charge transfer processes at multiphase interfaces including the solid state (catalyst, discharge products), the gaseous state (CO_2 gas), and the liquid state (electrolyte).[12,18] The elucidation of the basic reaction mechanism of LCBs offers a foundation for the reasonable battery system design. Several electrochemical reaction pathways are summarized in this section.

2.1 Li_2CO_3 and C discharge product system

Pure CO_2 gas used as the active material for the LCB cathode was reported by Archer's group for the first time,[20] which had a discharge capacity at 100 °C that was 10 times higher than the discharge capacity at 40 °C. *In situ* and non-*in situ* charac-

Haixia Chen

Ms Haixia Chen received her bachelor's degree in Materials Chemistry from Anqing Normal University in 2022 and then studied for Master's degree in Materials Science and Engineering at Nanjing University of Aeronautics and Astronautics. Her current research direction includes Li–CO_2 batteries and the application of photocatalysis.

Hairong Xue

Dr Hairong Xue received his B.S. (2009), M.S. (2012) and PhD (2016) degrees from the College of Materials Science and Technology, Nanjing University of Aeronautics and Astronautics (NUAA, China). He worked as a lecturer at the College of Chemical Engineering, Zhejiang University of Technology (ZJUT, China) after graduation. During 2018–2022, he worked in the group of Prof. Renzhi Ma at the National Institute for Materials Science (NIMS, Japan) as a Postdoctoral Fellow. Now he is a Professor at Zhongyuan Critical Metals Laboratory, Zhengzhou University. His research interest centers on developing functional materials for energy storage and conversion.

terization results showed that the discharge products were Li_2CO_3 and C. Eqn (1) for the total reaction was deduced as follows:

$$4Li + 3CO_2 \leftrightarrow 2Li_2CO_3 + C. \quad (1)$$

Subsequently, Chen's group[21] used the electrolyte of $LiCF_3SO_3$ in TEGDME (1 : 4 in mole) can realize the reversible discharge and recharge of LCBs. Drawing conclusions from X-ray diffraction (XRD) and Fourier transform infrared (FT-IR) spectra, the discharge product in the final state is Li_2CO_3 (Fig. 2a and b). In addition, they used porous gold as the battery cathode to avoid the effect of carbon presence on the characterization of discharge products, and the charge–discharge curve was similar to the Ketjen Black (KB)-cathode battery and found porous carbon by surface-enhanced Raman spectroscopy (SERS) and electron energy loss spectroscopy, which led to the proposal of a reasonable disproportionate reaction mechanism during the discharge stage of LCBs as shown in eqn (2)–(5):

$$2CO_2 + 2e^- \rightarrow C_2O_4^{2-} \quad (2)$$

$$C_2O_4^{2-} \rightarrow CO_2^{2-} + CO_2 \quad (3)$$

$$C_2O_4^{2-} + CO_2^{2-} \rightarrow 2CO_3^{2-} + C \quad (4)$$

$$CO_3^{2-} + 2Li^+ + Li_2CO_3. \quad (5)$$

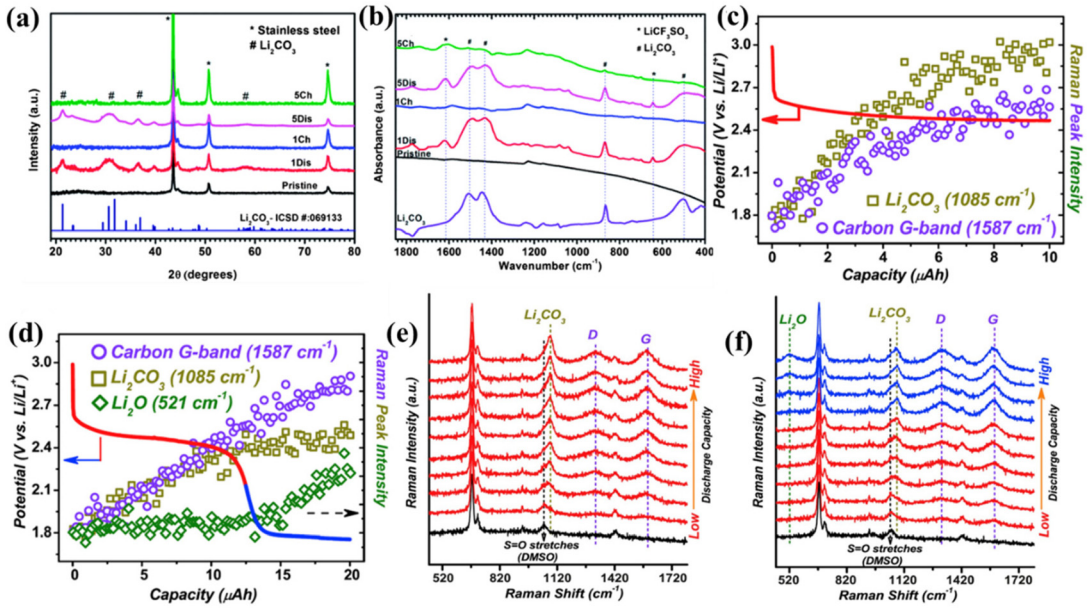

Fig. 2 (a) The XRD pattern and (b) FTIR spectra of the pristine KB electrode in LCBs.[21] Copyright 2014, the Royal Society of Chemistry. *In situ* surface-enhanced Raman spectra on gold electrodes with a current of 5 μA and capacities of (c) 10 μA h and (d) 20 μA h during discharge. The *in situ* Raman spectra related to capacity during the corresponding discharges of (e) 10 mA h and (f) 20 mA h.[22] Copyright 2017, Elsevier Inc.

Lulu Jia

Dr Lulu Jia received her bachelor's and master's degrees from the School of Materials Science, Central South University (CSU, China) in 2016 and 2019, respectively. She then pursued her PhD study in the group of Prof. Renzhi Ma and Prof. Yoshiyuki Sugahara at the National Institute for Materials Science (NIMS) in Japan and received her PhD from Waseda University in 2023. Her research interests focus on functional low-dimensional nanomaterials for energy conversion (e.g., electrocatalysis for hydrogen production) and energy storage (e.g., lithium-ion batteries).

Tao Wang

Dr Tao Wang received his PhD degree in Materials Physics and Chemistry from the Nanjing University of Aeronautics and Astronautics (NUAA) in 2012. From 2013 to 2015, he worked in Prof. Ye's group as a postdoctoral fellow at the National Institute for Materials Science, Japan. After that he took the associate professor position in NUAA. His current research interest focuses on the design, preparation, and application of porous materials for photoelectrochemical catalysis.

Subsequently, Zhou *et al.*[22] examined the trends of the components of Au-cathode LCBs by SERS in a non-protonic environment. Under CO_2 saturation conditions, the capacity was limited to 10 mA h, and a discharge plateau of 2.5 V was observed at a current of 5 mA (Fig. 2c). When the capacity was increased to 20 mA h, a new plateau was observed near 1.8 V (blue trace) as shown in Fig. 2d. According to the *in situ* Raman results (Fig. 2e and f), a new characteristic peak belonging to Li_2O is observed at 520 cm^{-1}. By comparing the changes in different substances after expanding the discharge capacity, Li_2CO_3 gradually decreases under the continuous deposition of Li_2O, while the growth of carbon seems to be unaffected. Here, it is mainly the change in discharge capacity that causes the continuous decay of the battery, the insufficient supply of CO_2 at 1.8 V, and the dynamic equilibrium of CO_2 in the bi-electrode layer that is controlled by the availability. Systematic experiments found that higher polarization potentials and local CO_2 concentration changes to be responsible for this shift.

Table 1 Possible reactions of Li_2CO_3 decomposition and the Gibbs free energies and reversible potentials of the corresponding reactions

No.	Possible reactions	E_{rev} [V] *versus* Li
I	$Li_2CO_3 \rightarrow CO_2 + \frac{1}{2}O_2 + 2Li^+ + 2e^-$	3.82
II	$Li_2CO_3 + \frac{1}{2}C \rightarrow \frac{3}{2}CO_2 + 2Li^+ + 2e^-$	2.80
III	$2Li_2CO_3 \rightarrow 2CO_2 + 4Li^+ + O_2^{\bullet-} + 3e^-$ $O_2^{\bullet-} \rightarrow O_2 + e^-$ $O_2^{\bullet-} \rightarrow O_2$ + electrolyte → uncertain product	Unknown value

As shown in Table 1, three thermodynamically possible reaction pathways for the electrochemical decomposition of Li_2CO_3 were summarized by Zhou's group in 2016.[23] They simulated discharged LCBs by pre-filling the electrodes with Li_2CO_3 and using ^{12}C and ^{13}C as conducting additives. They generated the gas composition produced during the charging of the prefilled electrode by *in situ* gas chromatography-mass spectrometry (GC-MS) measurements and isotope tracer methods. Fig. 3a(I) shows the charging curves of the two distinct batteries with ^{12}C and ^{13}C carbon in the Li_2CO_3 electrode charging curves and Fig. 3a(II–IV) show that the amount of all three substances increases at the beginning of the battery charging process, and decreases after charging, while no O_2 is released during the entire charging stage. According to the proposed pathway I, the self-decomposition of Li_2CO_3 generates CO_2 and O_2, while the GC-MS results showed that no O_2 was observed during the entire charging process, indicating that pathway I is not a reliable route for decomposition of Li_2CO_3. According to the mechanism proposed in Path II, C combines with Li_2CO_3 to precipitate CO_2 gas. The capacity of the two batteries is equal, and the battery using ^{13}C as a conductive additive produces one-third less $^{12}CO_2$ than the battery

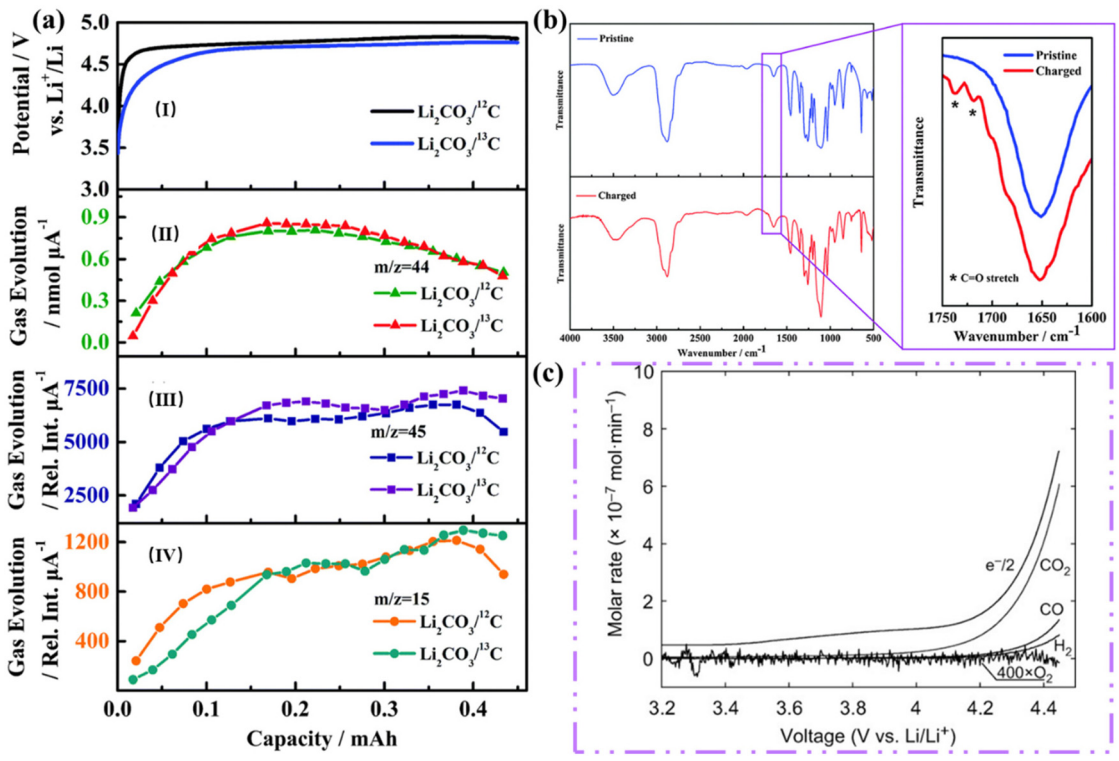

Fig. 3 (a) Charging curves of Li_2CO_3 electrodes in two different batteries with conductive additives of ^{12}C and ^{13}C. Gas evolution of CO_2 in the two batteries during charging ((II) (Fragment-44), (III) Fragment-45, and (IV) Fragment-15). (b) FTIR spectra of electrolyte solvents before and after charging.[23] Copyright 2016, The Royal Society of Chemistry. (c) Evolution of CO_2, O_2, CO, and H_2 from carbon black/Li_2CO_3/PTFE (9 : 1 : 1, m : m) composite electrodes during a linear potential scan of 0.14 mV s^{-1}.[24] Copyright 2018, Wiley-VCH GmbH.

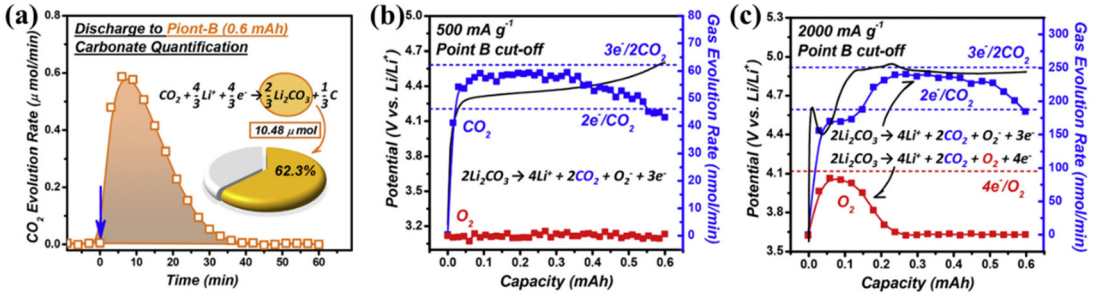

Fig. 4 (a) The evolution rate of CO_2 under carbonate quantification conducted on a cathode discharged at 0.6 mA h. DEMS results of CO_2 and O_2 evolution rates during the battery charging process at (b) 500 mA g^{-1}, and (c) 2000 mA g^{-1}.[22] Copyright 2017, Elsevier Inc.

using ^{12}C as a conductive additive. However, GC-MS shows that the emissions of ^{12}C and ^{13}C are almost equal, leading to the conclusion that Path II is not a reliable pathway. In addition, to simulate the chemical environment of pathway III, they used the complexation reaction between KO_2 and dicyclohexyl-18-crown-6, and fragments from the breakdown of the electrolyte solvent under the attack of superoxide radicals were also detected. The FT-IR results of the electrolyte solvent after simultaneous charging revealed stretching peaks located at 1720 cm^{-1} and 1737 cm^{-1} were judged to belong to the ester C═O stretch, consistent with the mechanism proposed for Pathway III. The absence of O_2 during the oxidative decomposition of Li_2CO_3 was also accounted for in a subsequent study (Fig. 3c).[24] Additionally, GC-MS was utilized to explore the discharge composition and gas oxidation in a more precise and quantitative manner (Fig. 4a–c). The analysis began with a quantitative assessment of Li_2CO_3 in the process of discharge using the CO_2 gas release rate from the cathode discharge after acid treatment. The deduced discharge reaction was found to be in excellent agreement with the reaction in eqn (1). During the subsequent charging process, the corresponding gas release rates at different current rates were analyzed using DEMS. At the beginning of the charging period, the release of CO_2 and O_2 could be detected at a high current rate (2000 mA g^{-1}, Fig. 4c), with charge-to-mass ratios of $2e^-/CO_2$ and $4e^-/O_2$, respectively, and it is proven that the decomposition of Li_2CO_3 is consistent with the formula: $2Li_2CO_3 \rightarrow 2CO_2 + O_2 + 4Li^+ + 4e^-$. Therefore, the decomposition of Li_2CO_3 into CO_2, O_2, and superoxide radicals is a convincing charging mechanism for LCBs.

2.2 Li_2CO_3 and CO discharge product system

Among the numerous reduction products of electrocatalytic CO_2 reduction, CO is an important industrial intermediate used in the chemical and metallurgical industries widely. Currently, great efforts have been made by researchers to explore efficient catalysts in the electrochemical reduction of CO_2 to CO.[25–27] CO gas generation in LCBs is therefore a technology that kills two birds with one stone by utilizing energy and converting it into a value-added product.

Archer's group concluded that $4Li + 3CO_2 \rightarrow 2Li_2CO_3 + C$ dominates during the discharge process of Li–CO_2 batteries,[20] but according to the potential from the initial value near the equilibrium potential to exceeding the theoretical equilibrium potential, which violates Tafel's theory. Meanwhile, the gas-phase composition of the LCBs was analyzed by DEMS. CO was not the major release, and it was assumed that CO disproportionately generated CO_2 and C during the discharge reaction. Xie *et al.* prepared three-dimensional porous zinc as the LCB cathode by redox-coupled electrodeposition. The discharge products were analyzed in both gaseous and solid states, and gas chromatography (GC) was used to find that CO was the main discharge product, and the undefined C was not detected. It is proposed that the mechanism responsible for the generation of the primary CO product is $2Li^+ + 2CO_2 + 2e^- \rightarrow CO + Li_2CO_3$ (Fig. 5a–c).[28] They confirmed the feasibility of

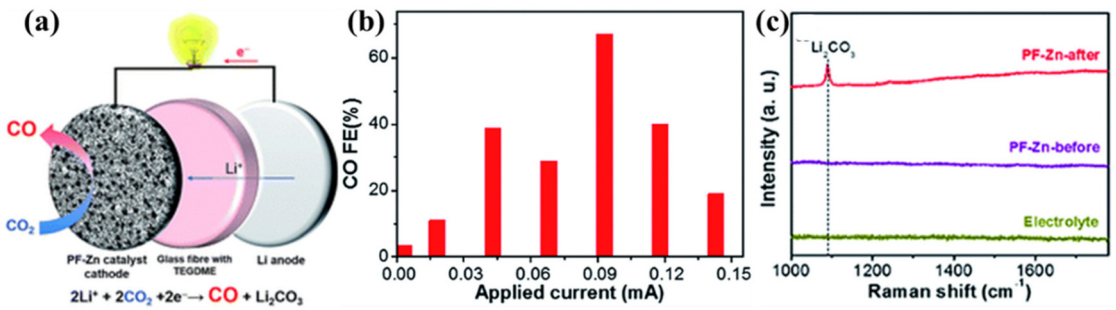

Fig. 5 (a) Schematic diagram of the porous Zn cathode for LCBs and its reaction mechanism. (b) Maximum FE of CO at several currents during 10 h of discharge. (c) Raman spectra of solid products on the PF-Zn cathode after discharge.[28] Copyright 2018, the Royal Society of Chemistry.

achieving efficient energy use by exploring high-value carbon-based products from metal–air batteries. The exact reaction mechanism needs to be further explored.

2.3 HCOOH discharge product system

As a discharge product of non-proton electrolyte LCBs, Li_2CO_3 is a wide bandgap insulator that is tough to decompose, which is a major obstacle to improving the electrochemical performance. Conversion of discharge products into other soluble liquid products is an attractive strategy to overcome this problem. Among them, formic acid discharge products are the most accessible among many liquid products, and metals such as In,[29] Sn,[30] and Bi [31,32] have been found to have high selectivity in the CRR. However, the formic acid product needs to be converted by binding to H^+ during the CRR, and the formic acid system is not applicable to aprotic LCBs.

Xue *et al.* used the strategy of attaching Li foils directly to inorganic LAGP solid-state electrolytes to realize aqueous LCBs while protecting the Li anode.[33] The porous Pd film prepared by electrodeposition on carbon paper facilitates the penetration and transport of electrolytes and CO_2 (Fig. 6a and c). Combined with the LAGP electrolyte, reversible cycling of CO_2 and soluble HCOOH during charging and discharging and an ultra-low overpotential were realized in aqueous-phase LCBs (Fig. 6b). The aqueous battery has a low overpotential of 0.38 V and a energy efficiency of up to 91%, and the recyclability of the battery has been demonstrated, offering a promising prospect for CO_2 conversion work and the application of LCBs. The discharge products of aqueous LCBs, HCOOH, are more susceptible to electrochemical decomposition relative to those of aprotic LCBs. They found that the charge potential for HCOOH oxidation is below 3 V and only CO_2 was oxidized out and there was no escape of O_2. This suggests that water decomposition is limited during the charging process of this battery, and a stable reversible cycle with high energy efficiency is achieved at lower overpotentials.

2.4 $Li_2C_2O_4$ discharge product system

Li_2CO_3, the main discharge product of LCB, limits the performance of the battery due to its wide band gap insulator properties and insolubility in non-protonic electrolytes, while $Li_2C_2O_4$, which is thermodynamically unstable and decomposes more easily compared to Li_2CO_3, has been studied as the LCB discharge product. Chen *et al.*[34] found that the reduction intermediate product $Li_2C_2O_4$ could be stabilized by Mo_2C during discharge and the formation of insulating Li_2CO_3 could be prevented, and concluded that a possible discharge reaction mechanism is shown in eqn (6) and (7).

$$2CO_2 + 2e^- \rightarrow {C_2O_4}^{2-} \quad (6)$$

$${C_2O_4}^{2-} + 2Li^+ + Mo_2C \rightarrow Li_2C_2O_4 + Mo_2C. \quad (7)$$

Mo_2C can stabilize the amorphous intermediate ${C_2O_4}^{2-}$ during discharge and decompose at low charging potentials (Fig. 6d), which can enhance the LCB round-trip efficiency. In addition, the combination of experimental and computational results has proved that the low-valent Mo atoms can form a Mo–O bond in Mo_2C to stabilize the discharge intermediate $Li_2C_2O_4$ of porous morphology and prevent it from further reacting to carbonate. In contrast, in the charging phase, the Mo–O bond is broken, and the discharge product is decomposed, which reduces the overpotential of the battery.[35] The ${C_2O_4}^{2-}$ is thermodynamically unstable, and the outer electrons (electron donors) of Mo_2C are transferred to the O atoms (electron acceptors) in $Li_2C_2O_4$ with structural optimization after adsorption, which ensures the rapid stabilization of the discharge intermediate by the electrons. The Mo_2C nanoparticles in Mo_2C@CC can play the role of an active center with high conductivity, effectively capture Li^+ and CO_2, promote the reaction, and realize a reversible LCB. The decomposition of the thermodynamically unstable discharge product $Li_2C_2O_4$ is shown in eqn (8). Sun *et al.* elucidated the $Li_2C_2O_4$ decomposition mechanism in LCBs in the presence of a redox mediator (RM).[36] During discharge, the Cu(I) RM-based electrolyte forms Cu(II)-oxalate adducts with the captured CO_2, and Cu(II)-oxalate adducts completely decompose after charging. Realization of $Li_2C_2O_4$ discharge products in LCBs is an ideal way to reduce charging potential and enhance reversible battery cycling.

$$Li_2C_2O_4 \rightarrow 2Li^+ + 2CO_2 + 2e^-. \quad (8)$$

2.5 Photo-assisted LCBs

The study of conventional electrocatalysts has gradually deepened, and it has been found that it is difficult to obtain a great reduction in the overpotential of these catalysts. Insufficient driving of CRR/CER by the catalyst is a key reason for the electrochemical performance of conventional LCBs. It was found that the introduction of light as a driver helps to realize efficient, stable LCBs.[13,37,38] Photocatalysts are capable of generating highly reducing-active photogenerated electrons and highly oxidizing-active photogenerated holes under light, which help to reduce the LCB overpotential, improve the electrochemical performance, and achieve light-assisted energy storage.[39–41] As shown in Fig. 7a, Guan *et al.* hypothesized that photoelectrons and holes segregate into the conduction and valence bands of the semiconductor and are transferred by the potential difference between the anode and cathode, respectively, helping to achieve the regulation of the discharge and charging potentials.[42] The choice of the photocatalyst is critical to optimize the efficiency and stability of these cells. Catalysts with appropriate bandgap energies ensure efficient light absorption and electron–hole pair generation, enhancing CO_2 conversion. High reactivity and chemical stability are the main influencing factors for repeated cycling of LCBs. In addition, simplicity of synthesis and compatibility with battery structures such as electrolytes are also important considerations in the selection of catalysts. A single photocatalyst of a certain type cannot satisfy the good electrical conductivity, superior catalytic activity, and chemical stability of the electrode material, and it needs to be modified by

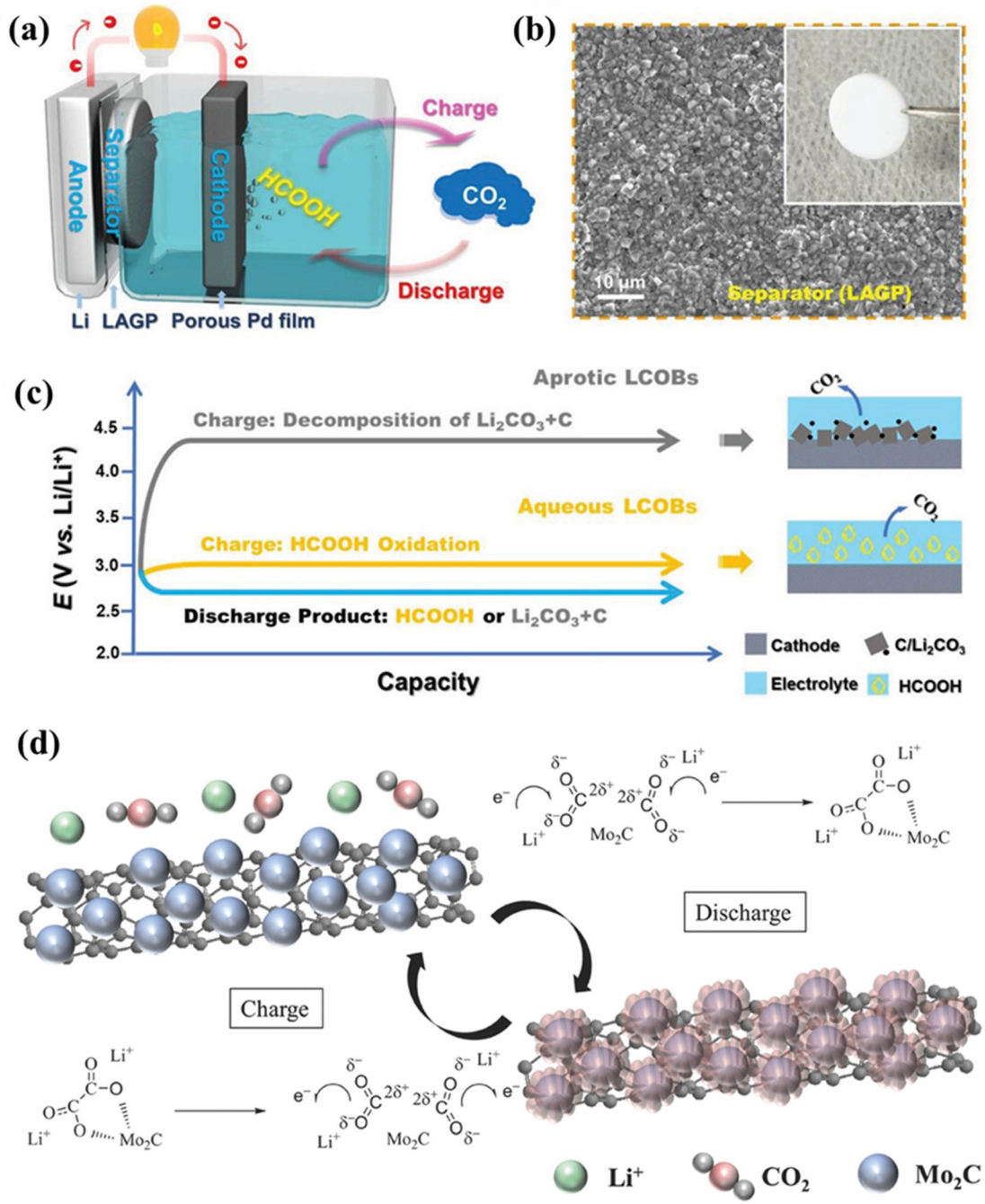

Fig. 6 (a) Schematic diagram and reaction mechanism of aqueous LCBs. (b) SEM image and photograph (inset) of the LAGP separator. (c) Comparison of aqueous LCBs with conventional aprotic LCBs.[33] Copyright 2021, Wiley-VCH GmbH. (d) Schematic diagram of the charge/discharge reaction of the Mo_2C/CNT cathode in LCBs.[34] Copyright 2017, Wiley-VCH Verlag GmbH & Co. KGaA, Weinheim.

various means. Various types of photocatalysts have been developed for application to LCBs, including photovoltaic semiconductors,[42] noble metal loadings,[13] and MOF materials.[38] Attempts were made to combine photoelectric semiconductors with various types of collectors to form composites, obtaining photocatalysts with stronger conductivity and better catalytic activity. The cathode catalyst for LCBs could accelerate charge transfer during battery cycling and improve battery retardation kinetics. The effective expansion of the range of light absorption by noble metal materials can help the photoelectric semiconductor to play an efficient catalytic role under visible light or even infrared light, accelerate the directional migration of photogenerated electrons and holes, and obtain better photoelectrocatalytic activity. At present, the participation of photogenerated carriers in the charge/discharge reaction mechanism of photo-assisted LCBs

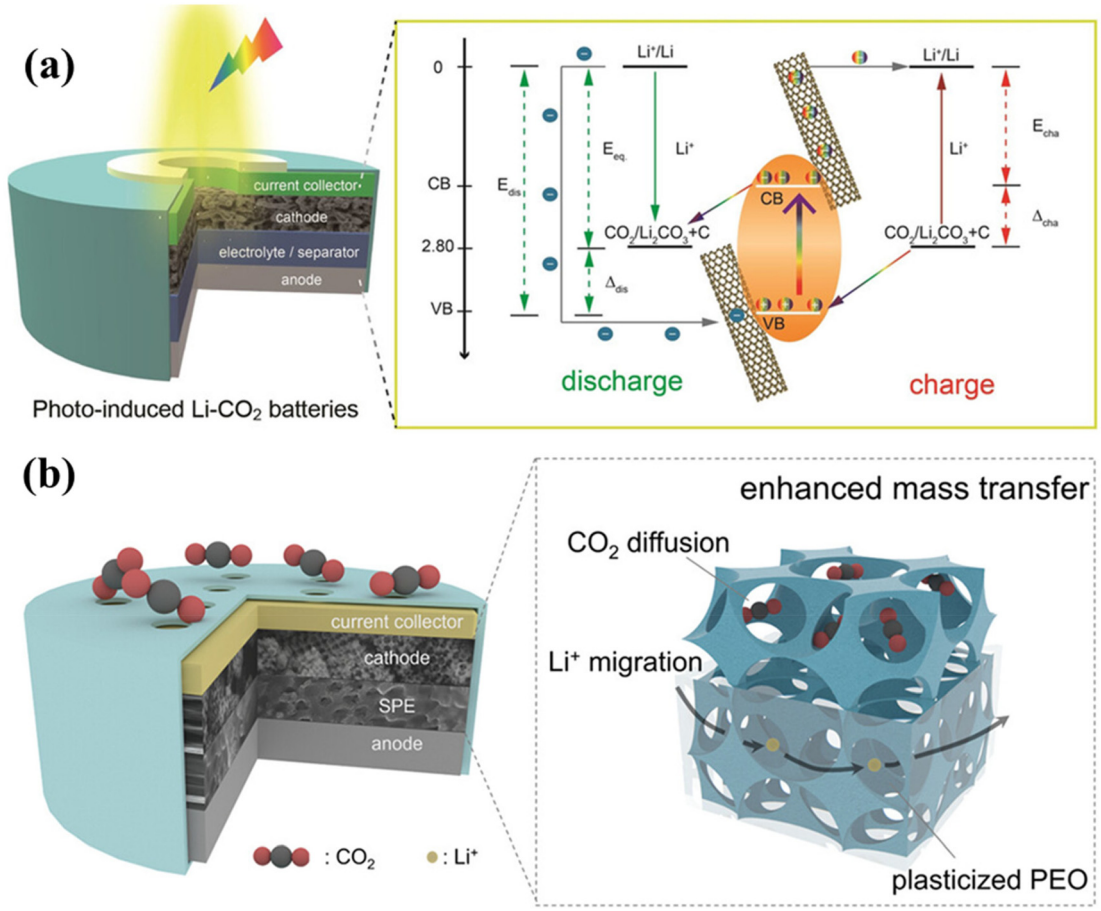

Fig. 7 (a) Basic structure and energy level schematic of photo-assisted LCBs for improved electrochemical performance under illumination.[42] Copyright 2020, Wiley-VCH GmbH. (b) Multi-phase mass transfer schematic in all-solid-state LCBs.[43] Copyright 2024, American Chemical Society.

is still confined to the electrocatalytic environment, and further research elaboration is essential.

2.6 All-solid-state LCBs

Currently, research on LCBs is mainly concentrated on liquid systems. However, liquid electrolytes may volatilize and decompose during battery cycling, threatening the safety performance of batteries due to their flammability and volatility. Therefore, solving the problem of electrolyte volatilization is a necessary approach to improve the safety performance of LCBs. The high ionic conductivity and excellent mechanical properties of all-solid-state LCBs have already served as an ideal solution to the above challenges.[44–46] Meanwhile, batteries using solid-state electrolytes will not require a long activation process, which can reduce step times in mass production and increase productivity. Solid electrolytes are a class of solids that conduct specific ions. The ionic conductivity of different types of solid electrolytes varies somewhat and changes with temperature. Polymer solid electrolytes are formed by dissolving lithium salts in polymers. Polymer electrolytes of systems such as poly(vinylidene fluoride), poly(phenylene nitrile), poly(ethylene chloride), and poly(ethylene oxide) have been developed and studied. Polymer solid-state electrolytes are flexible enough to accommodate volume changes during battery operation, providing new strategies for wearable electronic devices.[47,48] Zhao *et al.* constructed a bi-continuous hierarchical porous structure while utilizing macro-microporous zeolitic imidazolate framework-8 (OM-ZIF-8) as a dopant for polymer electrolytes and as a battery cathode (Fig. 7b).[43] The interconnected macropores in OM-ZIF-8 facilitated mass transfer in all connecting directions in the polymer electrolyte and anode, maintaining a high ionic conductivity. Mushtaq *et al.* prepared a three-dimensional mesh-structured polymer electrolyte with an ionic conductivity of up to 3.6×10^{-4} S cm^{-1} at room temperature by cross-linking modified silica-terminated polyether-based PEs, and the assembled LCBs can be cycled more than 100 times at 100 mA g^{-1}.[49] Solid inorganic electrolytes can exhibit higher Li^+ transport efficiency and chemical and thermal stability relative to polymer electrolytes. A wide variety of inorganic solid electrolytes, including oxide-based materials, sulfide-based materials, and halide-based materials, were used. Among them, the sodium superionic conductor (NASICON), which has excellent chemical stability, has received much attention. The structure of NASICON-type electrolytes can be represented by $LiM_2(PO_4)_3$ (M = Ti, Ge, Zr), which has a polyhedral structure that establishes fast ion transport channels and enhances conductivity. Moreover, both doping

with covalent elements and heterovalent doping can be achieved to enhance Li ion mobility. Polymer electrolytes have a flexible morphology but insufficient room temperature conductivity and poor stability, while solid-state inorganic electrolytes have high electrochemical stability and ion transport velocity but lack good elasticity and flexibility. Combining the two to achieve better ion transport and improve the ability to adapt to the volume change of solid-state composite electrolytes provides a new idea in solid-state battery research and development. Garnet-based solid-state electrolytes with higher ionic conductivity and stability to lithium are a premium choice for future solid-state lithium–air batteries. Wang *et al.* introduced $Li_7La_3Zr_{1.4}Ta_{0.6}O_{12}$ into polyethylene oxides to form a composite solid-state electrolyte, the cycle life of assembled batteries increased.[44] Unfortunately, the garnet-type electrolyte reacts easily with water and CO_2 in air to form a layer of inert material on the surface of the electrolyte, and the practical application of batteries is hindered.

The development of all-solid-state LCBs is still at an early stage. The internal design and assembly of the components are critical to achieve stable and efficient operation of all-solid-state LCBs. The combined construction of the cathode, anode, solid electrolyte, separator, and collector requires special attention. With particular attention to the choice of solid electrolyte which plays a crucial role in preventing the formation of dendrites, improving safety, and stabilizing the battery electrochemical reactions. In terms of the integrity and overall performance of the battery, a strong battery casing with a solid sealing condition is an important foundation. Solid-state electrolyte research also needs to consider the ion transport and interfacial contact issues over a wide electrochemical window and operating temperature, and the protection of the anode-solid-state electrolyte interface. The performance enhancement of cathode catalysts, lithium anode corrosion and dendritic problems also need to be faced by all-solid-state LCBs.

3. Classification of catalysts

Compositional tuning of catalysts is important to facilitate the development of high-performance LCBs. Changing the composition and material ratio of catalysts enhances the catalytic activity and selectivity by optimizing the surface properties and electronic structure. Meanwhile, the addition of some components can also alleviate the battery aging problem and reduce the overpotential. In addition, adjusting the battery construction and utilizing the synergistic effect between components can achieve the purpose of improving the overall electrochemical performance. It is crucial to design efficient electrocatalysts and photocatalysts to accelerate the slow kinetics of the CRR/CER process, extend the cycle life, and realize a stable and reversible cycle of the battery. Currently, a massive amount of work has been carried out on the research of catalysts. In this section, the performance and mechanism of LCBs of different catalysts will be summarized.

3.1 Carbon-based catalysts

Carbon-based materials with inherent characteristics including high electrical conductivity, a large specific surface area, and high surface active sites, and carbon materials including KB, graphene, carbon nanotubes, and carbon quantum dots were used as active materials in a broad range of applications in the field of energy storage and conversion devices.[50–52] Early researchers attempted to use commercial carbon materials as cathode catalysts for LCBs. However, due to the lower catalytic performance and a single limited structure, often undesirable electrochemical properties are obtained. Zhang *et al.* used graphene as a cathode in LCBs first,[53] and the battery performance showed a very significant improvement in comparison with KB, and this battery exhibited superior battery capacity and excellent cycling stability. Zhang *et al.* introduced carbon nanotubes (CNTs) into the reversible LCBs in the same year.[54] They found that the 3D network structure of CNTs promotes electron transfer and gas transport in addition to positively affecting the deposition of the discharge products. The electrochemical stability of the LCBs is significantly enhanced.

The performance of pure carbon materials in the CRR/CER reaction process is not satisfactory,[21] which limits the application and promotion of carbon materials in LCBs to some extent. However, modifying pure carbon materials by some means, such as functionalized doping and ports or defects, can create more active sites,[55–57] effectively improving the catalytic efficiency. Heteroatom (such as N, B, and other atoms) doping is an effective approach to address the catalytic inertness of pure carbon materials.[58–61] Li *et al.* prepared standalone, binder-free cathodes for LCBs, which aligned N-doped carbon nanotube (VA-NCNT) arrays on titanium wires (Fig. 8a).[55] The VA-NCNT arrays consist of thousands of vertical CNTs with a high N doping rate, abundant defects and void space as cathode catalysts. Due to the properties of these arrays, diffusion and penetration of CO_2 and electrolytes, the number of active sites, and the accumulation and decomposition of discharge products are facilitated (Fig. 8c). The assembled battery exhibited an excellent cycle life of 2520 h at 500 mA g^{-1} (Fig. 8b). Sun *et al.*[57] introduced inert boron nitride (h-BN) into graphene catalysts to constitute the BN-GN vdWsH material by using a ball-milling–annealing process. It was shown by experiments and theoretical calculations that h-BN could modify the electronic properties of graphene and exhibit excellent CRR and CER performances in LCBs. Meanwhile, the cycle life is more than three times longer.

Yu *et al.* designed free-standing N-doped graphene carbon aerogels with specific oxygen groups as cathodic catalysts under the guidance of theoretical simulations.[56] DFT calculations confirm that the electronic structure of graphene changes upon N doping, and the free energy of the reaction process is reduced. The CO_2-related intermediates can be further stabilized through the synergistic interaction of the inherent oxygen-containing functional groups of graphene aerogels with nitrogen dopants. Meanwhile, the three-dimensional hierarchical pore structure of the graphene carbon

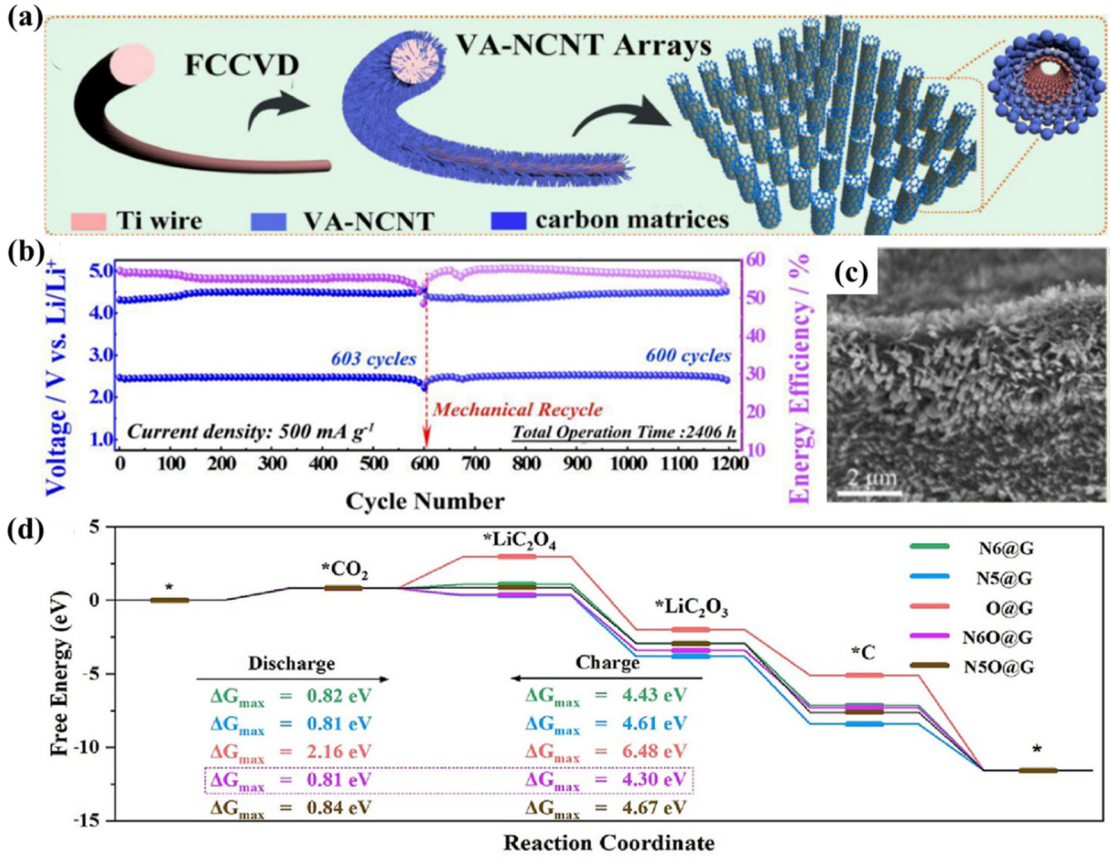

Fig. 8 (a) The process of synthesis of VA-NCNT arrays on titanium wires by the FCCVD method. (b) Cycling performance of the VA-NCNT array cathode at 500 mA g^{-1}. (c) SEM image of VA-NCNT arrays grown on Ti.[55] Copyright 2020, Elsevier Inc. (d) Gibbs free energy charts during the discharge–charge process in four models.[56] Copyright 2023, Elsevier Inc.

aerogel ensures good electrical conductivity while providing a high surface area, exposing accessible active sites. The improved catalytic activity and reaction kinetics of the CRR and CER were attributed to this N and O diatom-doped catalysts (Fig. 8d). The results show that the assembled LCB maintains cycling stability for over 1500 h while showing a higher initial energy efficiency of approximately 78.46%. Additionally, carbon quantum dots (CQDs) demonstrate new trends in emerging hot research due to their large number of edge defects and quantum confinement.[62–64] However, the electrocatalytic activity of CQDs is limited by poor electrical conductivity. Dai's group designed a composite catalyst consisting of porous graphene-supported carbon quantum dots (CQD/hG) with a π–π stacking structure.[65] The edge defects around the electrodes of the CQD/hG composites offer a vast number of active sites for charge and discharge.

Currently, photo-assisted LCBs are considered to be an effective way to accelerate slow electrochemical kinetics. It was found that defect-rich semiconductor materials exhibit improved catalytic activity relative to well-crystallized materials. Li *et al.* designed carbon nitride coated with nitrogen defects on interwoven CNT conductive scaffolds (CNT@C_3N_4) as a heterostructured photovoltaic cathode.[14] The unique defect structure of C_3N_4 enables it to efficiently collect UV-visible light, generating abundant carriers ensuring photogenerated electrons and holes to drive the CRR/CER reaction. The assembled batteries achieve an ultra-high energy efficiency of 98.8% and an ultra-low polarization value of only 0.04 V. In 2017, Hu *et al.* reported a solid-state LCB based on a composite polymer electrolyte@CNT cathode, with 100 stable cycles and a flexible pouch battery capable of cycling for more than 200 h at different degrees of flexing.[66]

Overall, carbon-based materials are a class of catalytic materials with excellent electrical conductivity, abundant sources, and low cost. They have been applied widely in the design of cathode materials for many types of batteries, and some breakthroughs of structural design and heteroatom doping have been achieved. However, the existence of carbon materials itself limits the characterization of the batteries' charging/discharging process and reaction mechanism. The catalytic effect of carbon-based materials alone is not enough to promote the decomposition of the discharge products. Therefore, research on more effective catalysis to solve the problem is needed.

3.2 Noble metal-based catalysts

Precious metals and their composites have been studied extensively and applied in various fields, due to their unique elec-

tronic configuration and excellent electrochemical activity, stability, and selectivity.[36,67] Noble metal materials have been continuously covered as cathodic catalysts for LCBs in recent years.[68,69] In 2017, Zhou's group first introduced precious metals into LCBs,[70] and they deposited Ru nanoparticles on Super P by the solvothermal method. Ru@Super P exhibited excellent electrocatalytic activity, the charging potential of the assembled battery was significantly reduced, and it was able to be stably cycled 80 times. Considering the excellent catalytic properties of Ru in LCBs, Lin *et al.* developed a catalyst for LCBs that utilizes N-doped carbon nanoboxes as the substrate, combining Ru-atom clusters (RuACs) and single-atom Ru–N_4 (Ru_{SA}) composite sites.[71] The Ru_{AC+SA}@NCB exhibited excellent catalytic activity for CRR and CER, which enabled LCBs with unprecedentedly low overpotentials and excellent cycling stability. The overpotentials of LCBs using Ru_{AC+SA}@NCB as a cathode catalyst were 1.65 and 1.86 V at high current densities of 1 and 2A g^{-1}, respectively. The Ru_{AC+SA}@NCB catalyst enabled the LCB to reach a cycle life of 230 h (Fig. 9a and b). The enhanced catalytic capacity stems from the fact that the adjacent RuAC components substantially alter the electronic structure of the Ru–N_4 active site. The RuAC substance modulation of the electronic structure of Ru–N_4 sites optimizes the interaction with key intermediates, leading to reduced energy barriers in the CRR and CER rate-determining steps, and facilitating battery kinetics (Fig. 9c–e).

Wang *et al.* designed a synergistic catalyst of bis-precious metals combined with nitrogen-doped carbon nanotubes (IrRu/N-CNTs), which exhibited unique alloy dual-catalytic site properties in batteries.[72] The three-dimensional conductive network of IrRu/N-CNTs was consistent with that of N-CNTs from scanning electron microscopy (SEM) and transmission electron microscopy (TEM) images. This conductive network facilitated accelerated electron transfer and complete wetting of the electrolyte (Fig. 10a–e). Due to the synergistic effect of the Ir–Ru dual catalytic sites, the discharge capacity and cycle life of the battery were significantly improved, reaching 7660 h at a capacity of 500 mA h g^{-1} (Fig. 10j). The deposition and decomposition of thin film-like discharge products are promoted in the presence of the alloy catalyst. The electronic structure is effectively altered and the electron transfer pathway is shortened, resulting in excellent electrochemical performance (Fig. 10f–i). Wu *et al.* proposed the dispersion of IrO_2 nanoparticles on the N/CNT surface (IrO_2-N/CNT) and the active site density was improved.[73] The battery was able to achieve a capacity of 4634 mA h g^{-1}, an ultra-low charging plateau (3.95 V), and a long cycle life for over 2500 h.

Wang *et al.* attached RuO_2 particles to carbon textile-based TiO_2 nanoarrays as stand-alone positive electrodes for LCBs with satisfactory electrochemical performance.[74] Based on the three-dimensional stabilized array of TiO_2 and the catalytic property of RuO_2, the system LCBs could be cycled 238 times at 250 mA g^{-1}. By combining a noble metal with a semiconductor as a photocathode for photo-assisted LCBs, the photovoltaic effect of the semiconductor combined with the equi-excited exciton effect of the noble metal exhibits a stronger light trapping range, while reducing carrier complexes. Zhang *et al.* reported a TiO_2 nanotube array cathode modified

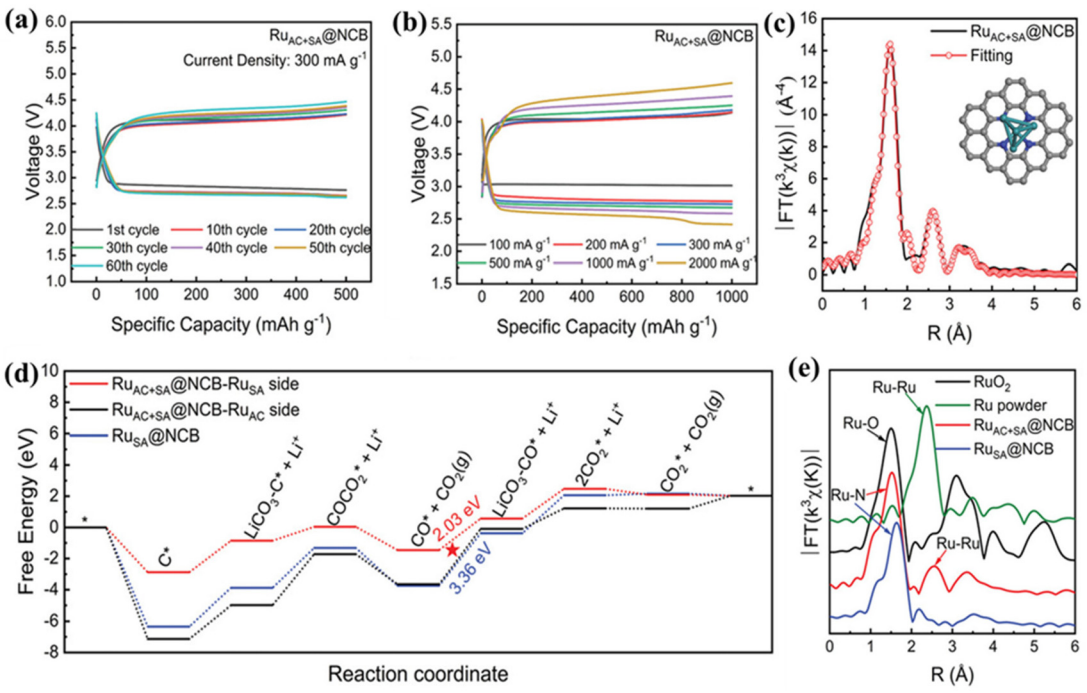

Fig. 9 (a) Voltage profile of the Ru_{AC+SA}@NCB cathode at 300 mA g^{-1}. (b) The rate performance of the Ru_{AC+SA}@NCB cathode at a current rate ranging from 100 to 2000 mA g^{-1}. (c) EXAFS fitting curves in the *R* space of the Ru_{AC+SA}@NCB. (d) Gibbs free energy diagrams during the CER process. (e) FT-EXAFS spectra in the *R* space of RuO_2, the Ru powder, the Ru_{AC+SA}@NCB, and the Ru_{SA}@NCB.[71] Copyright 2022, Wiley-VCH GmbH.

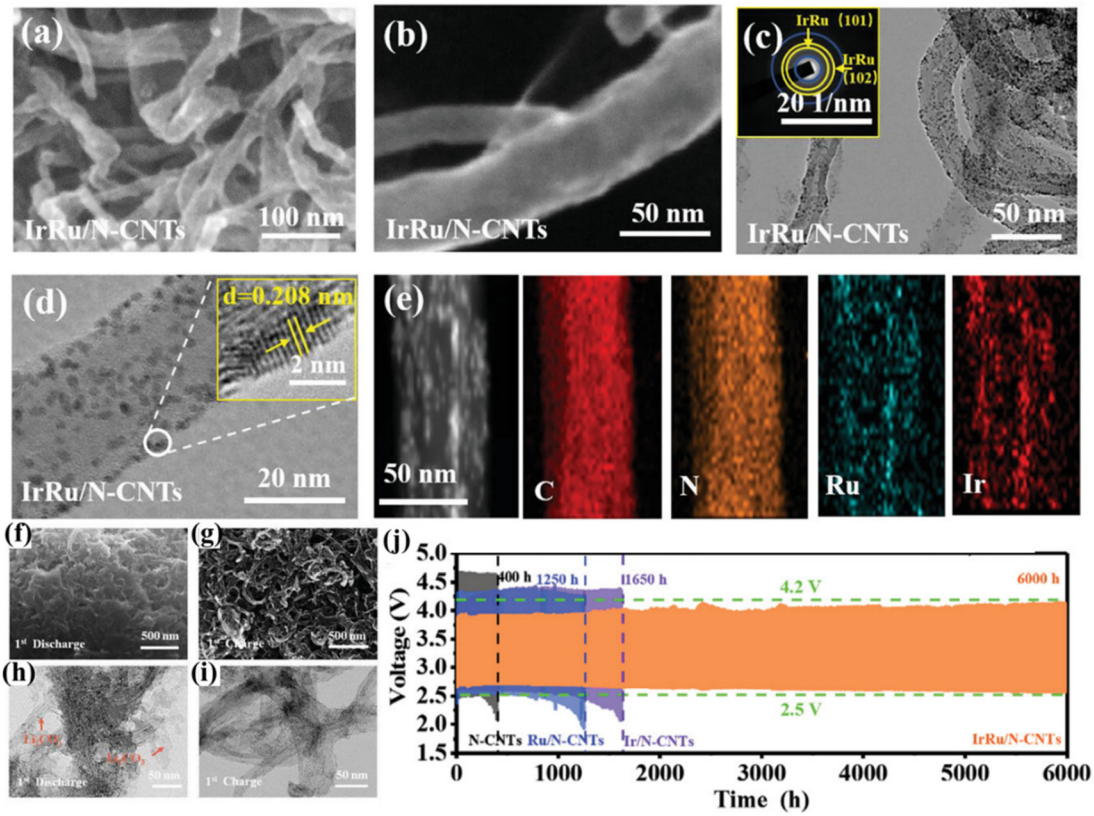

Fig. 10 (a and b) SEM images of IrRu/N-CNTs. (c) TEM images and the inset is the corresponding SAED pattern. (d) TEM images and the inset is the HRTEM image of alloyed IrRu nanoparticles. (e) TEM image of IrRu/N-CNTs and the corresponding EDX elemental mapping images. SEM images of the fully (f) discharged and (g) recharged IrRu/N-CNT cathode. The TEM images of the IrRu/N-CNT cathode fully (h) discharged and (i) recharged. (j) The voltage/time curves of the IrRu/N-CNTs cathode at 100 mA g^{-1} at a cutoff capacity of 1000 mA h g^{-1}.[72] Copyright 2023, Wiley-VCH GmbH.

with Ag nanoparticles.[13] The dual-field-assisted cathode combining the photoelectric effect and plasma action produced by this semiconductor photocatalytic material helps to break through the barrier of the slow kinetics of the CRR/CER. Collective oscillations of free electrons excited by the plasma of Ag nanoparticles resonate with the incident light to promote the scattering and absorption of incident light energy by spherical nanoparticles. Scattering of Ag nanoparticles enhances the absorption of the applied light energy by TiO_2, and more electrons and holes are generated (Fig. 11b and c). In addition, the absorption of incident light energy by Ag nanoparticles enhanced the local electric field around them. The enhanced local electric field promotes the photogenerated carrier separation and transfer, effectively utilizing the strong oxidizing properties of photogenerated holes and the excellent reducing properties from photogenerated electrons to accelerate the CRR/CER (Fig. 11d). $Li_{1.4}Al_{0.4}Ti_{1.6}(PO_4)_3$(LATP) and $Li_{1.5}Al_{0.5}Ge_{1.5}(PO_4)_3$ (LAGP) have excellent air stability and are the most widely studied solid-state electrolytes in Li–air batteries. Na *et al.* utilized a NASICON structured solid-state electrolyte and a Ru catalyst combined with multi-walled CNTs to improve battery safety and electrochemical performance.[15] A NASICON structured solid-state electrolyte of the class of LATP was used in the study for higher electrical conductivity, and superior CO_2 stability. The incorporation of Ru nanoparticles drastically reduced the voltage of the CO_2 oxidation process from 4.57 V to 4 V (Fig. 12c). The uniform deposition and rapid decomposition of the products fully confirm the reversible process of the battery. The LATP electrolyte powder has high uniformity and its high ionic conductivity improves the kinetic process of the battery, resulting in a higher capacity and longer cycle life (Fig. 12a and b). Xu's group combined the LAGP electrolyte and Au@TiO_2 catalyst to design an LCB with a wide temperature range.[16] Au nano-ions with a high surface plasmon resonance effect help to utilize the full spectrum range of solar energy more efficiently and accelerate the CRR/CER. Additionally, the combination of LAGP's excellent electrical conductivity with the photocatalyst achieves superior ion transport and thermal conductivity in the battery cycle. The battery can operate over an extremely wide temperature range (−73 to 150 °C), and even at temperatures of −73 °C (Fig. 12d and e), the batteries can exhibit a polarization of only 0.6 V aided by heat energy. Savunthari *et al.* reported that the Ru/CNT/LAGP system significantly improved the flexible synthesis and decomposition of the discharge products and exhibited stable cycling behavior for over 45 cycles.[75]

Currently, reported discharge voltages of all-solid-state LCBs are still higher than 4.0 V, and the higher polarization is

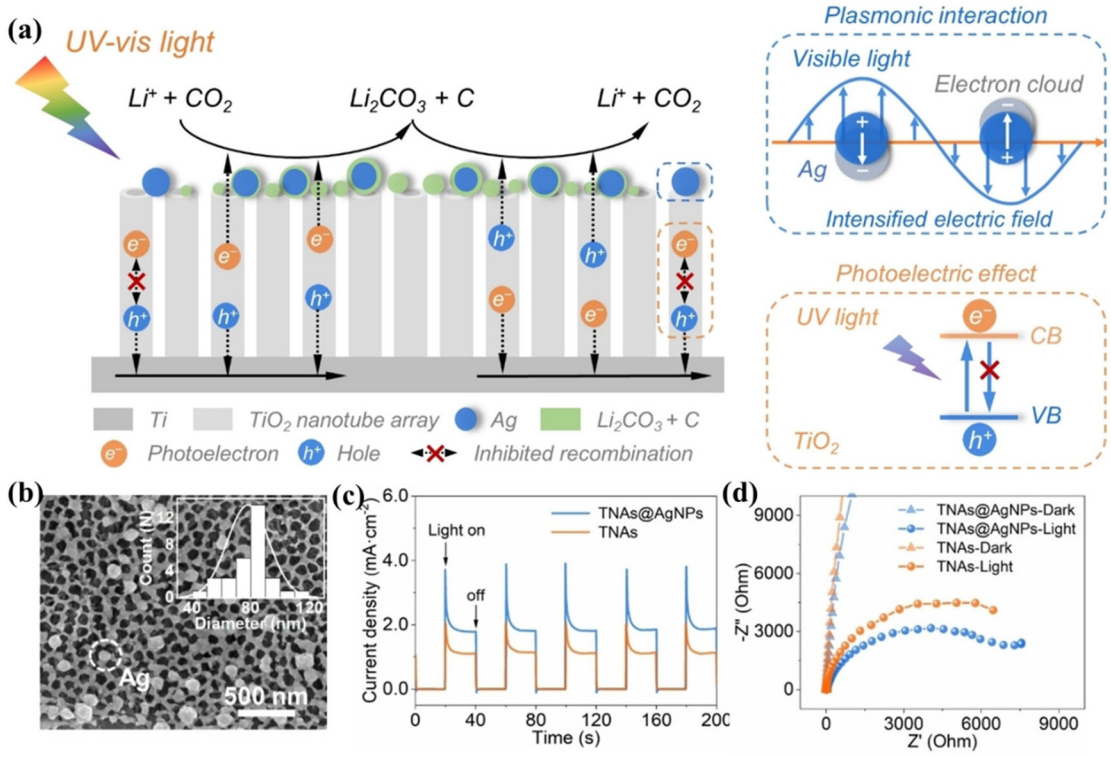

Fig. 11 (a) The diagram of the mechanism of the dual-field assisted Li-CO_2 battery. (b) TEM images of TNAs@AgNPs. (c) Photocurrent/time curves of TNAs and TNAs@AgNPs. (d) Electrochemical impedance spectra of TNAs and TNAs@AgNPs.[13] Copyright 2022, Wiley-VCH GmbH.

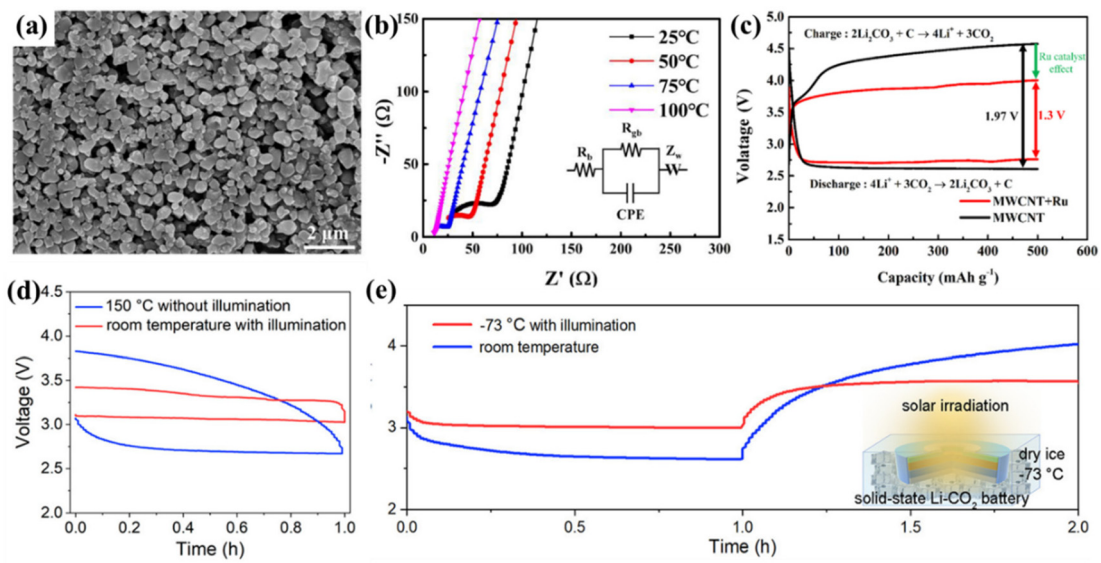

Fig. 12 (a) SEM image of the LATP powder. (b) Nyquist plots at several temperatures with equivalent circuits. (c) The polarization comparison curves of MWCNT and MWCNT/Ru batteries at 50 mA g^{-1}.[15] Copyright 2023, Elsevier. (d) The first discharge and charge curves of the all-solid-state LCBs at room temperature with light and 150 °C without light at 0.01 mA cm^{-2}. (e) First discharge and charge curves of the all-solid-state LCBs at room temperature and −73 °C with light at 0.01 mA cm^{-2}.[16] Copyright 2022, American Chemical Society.

not conducive to the stability of the batteries. Photogenerated electrons and holes produced by photocatalysts under light conditions facilitate the CER/CRR processes.[76] Therefore, the introduction of a light field in an all-solid-state LCB is considered as an effective method to exhibit electrochemical properties while ensuring safety.[77,78] Wang *et al.* introduced a light field in a solid-state LCB, which efficiently utilizes photogenerated carriers and exhibits an ultra-long cycle life and low

charge overpotentials.[17] Plasma Ru nanoparticle catalysts activate CO_2 molecules adsorbed during the discharge process to accelerate the breaking of C–O bonds and facilitate the discharge process. This is attributed to the non-homogeneous structure formed between the Ru catalyst and the discharge product Li_2CO_3, while the carriers generated by photothermal catalysis accelerate the process of CO_2 oxidative precipitation. An artificial molten salt interface (MSI) improves contact and stability between interfaces, and MSI solid-state LCBs with an ultra-low charge voltage of 2.95 V and excellent cycling stability for 450 cycles under photothermal assistance were obtained.

The excellent catalytic activity and stability of noble metals enable them to be used as catalysts for LCBs to effectively reduce polarization, exhibit outstanding electrochemical performance, and stable long-term cycling characteristics. However, the use of noble metals as catalysts for LCBs would greatly increase the cost of the batteries, making their industrialization difficult, and one of the central issues in noble metal catalyst design is to improve their efficiency.

3.3 Transition metal compound-based catalysts

Noble metals are effective in improving the energy efficiency of LCBs. However, the high cost hinders scientific research in this area. Transition metal materials are more suitable for practical application due to their availability and price. Additionally, transition metals have empty orbitals in their outer layer with unfilled electrons,[79] allowing them to easily undergo redox reactions by gaining or losing electrons. This characteristic has attracted the attention of scientific researchers.[80,81] Catalysts with metal single-atom-N_x groups can assist in improving LCB kinetics and increasing the battery cycling capacity.[82,83] Liu *et al.* used DFT to calculate the potential of N-doped graphene piggybacked with monometallic atomic materials (Me = Cr, Mn, Fe, Co, Ni, and Cu) for CRR/CER.[84] Among these materials, an N-doped graphene (NG) supported metal single-atom catalyst (SACr@NG/PCF) is considered to be the most effective reversible catalyst. As a validation of DFT calculations, the researchers affixed SAMe@NG to nickel foam without a binder. They also proposed "proton screening" to prevent the metal from a high mass loading during the annealing process and confirmed the structure of metal-N_4 by a series of characterization techniques. The SACr@NG/PCF cathode exhibits high CO_2 trapping and Li_2CO_3 decomposition capacity, and excellent rate performance. It has a low charge/discharge gap of 1.39 V and can be cycled up to 350 times at 100 μA cm^{-2}.

Metal single atoms are loaded on the surface of the carriers in the form of covalent coordination, and the interaction between the ligand and the carrier makes it an efficient catalyst.[85,86] Recently, Xu *et al.* anchored Cu single atoms on nitrogen-doped graphene as reversible catalysts for stable LCBs.[87] Benefiting from the covalent effect induced by the Cu–N_4 coordination results, the configuration of the charge density difference on the NG surface is altered, enhances the interaction between SA–Cu–NG and CO_2, and promotes the transfer of electrons from CO_2 to the active site of SA–Cu–NG. During the CER process, SA–Cu–NG has thermodynamic advantages over NG in the decomposition of Li_2CO_3 to achieve reversible LCBs with low polarization.

Transition metal oxides have semiconducting properties and represent a class of high-performance catalysts with great potential.[88–90] Deng *et al.* introduced a graphene aerogel as a scaffold to immobilize Co-doped CeO_2 nanosheets as a self-supporting binder-free LCB cathode.[91] Strongly coupled nano-interactions between CeO_2 and Co_3O_4 reorganized the electronic structure, enhanced CO_2 adsorption, and accelerated the decomposition process of the discharge products. The porous self-supported cathode facilitates the rapid diffusion of the electrolyte. The assembled battery has an excellent discharge capacity (7860 mA h g^{-1}) and a cycle life of more than 100 cycles.

With unique physicochemical properties, low price, and high stability, transition metal sulfides have been explored in photocatalysts, electrocatalysts, and Li–O_2/CO_2 batteries.[92,93] Lu *et al.* designed a V-MoS_2/Co_9S_8 heterostructure that is vertically anchored on carbon paper.[94] In this structure, the fully exposed MoS_2 grows on the highly active sites of Co_9S_8, which is supported by the carbon paper. The material exhibits a porous sheet-like structure, which serves as a platform for the transport and diffusion of CO_2 and electrolytes. Additionally, the discharge products are uniformly distributed under the action of abundant active sites. Notably, the complementary effect of the fully exposed MoS_2 rim and Co_9S_8 active sites reduces the energy barrier of the rate-determining step of the CRR, thereby exhibiting excellent intrinsic activity. The experimental results show a low potential of 0.68 V, with a high energy efficiency of up to 81.2%. Guan *et al.* designed a porous layered In_2S_3@CNT/SS as a bifunctional catalyst for flexible photo-assisted LCBs.[42] They proposed a new CO_2 activation strategy by first reducing In^{3+} to In^{+} under light and subsequently combining it with CO_2 reduction products to form the intermediate In^{3+}–$C_2O_4^{2-}$. The discharge process of LCBs was facilitated and the transformation from photo energy to electrical energy was realized. Moreover, they proposed a SiC/RGO composite catalyst to regulate the photogenerated electrons and holes by the joint action of RGO and SiC.[95] The battery CRR kinetics and the decomposition of the discharge product were accelerated, effectively realizing the photo-assisted low overpotential of LCBs.

Transition metal nitrides exhibit excellent electrical conductivity and low impediment to ion/electron transport due to their crystal structure, which is similar to that of the corresponding metal monomers. Transition metal nitrides have a variable and adjustable morphology, which provides a superior structure for ion/electron transport and storage.[96] In addition, transition metal nitrides have ultra-high stability and can maintain their structures and chemical compositions during long-term cycling processes.[97] Therefore, transition metal nitrides show great promise for applications in electrocatalysis and metal–air batteries.[98–101] Qi *et al.* proposed a binder-free cathode catalyst with MoN loaded on carbon cloth, which achieved faster reaction kinetics and higher energy efficiency

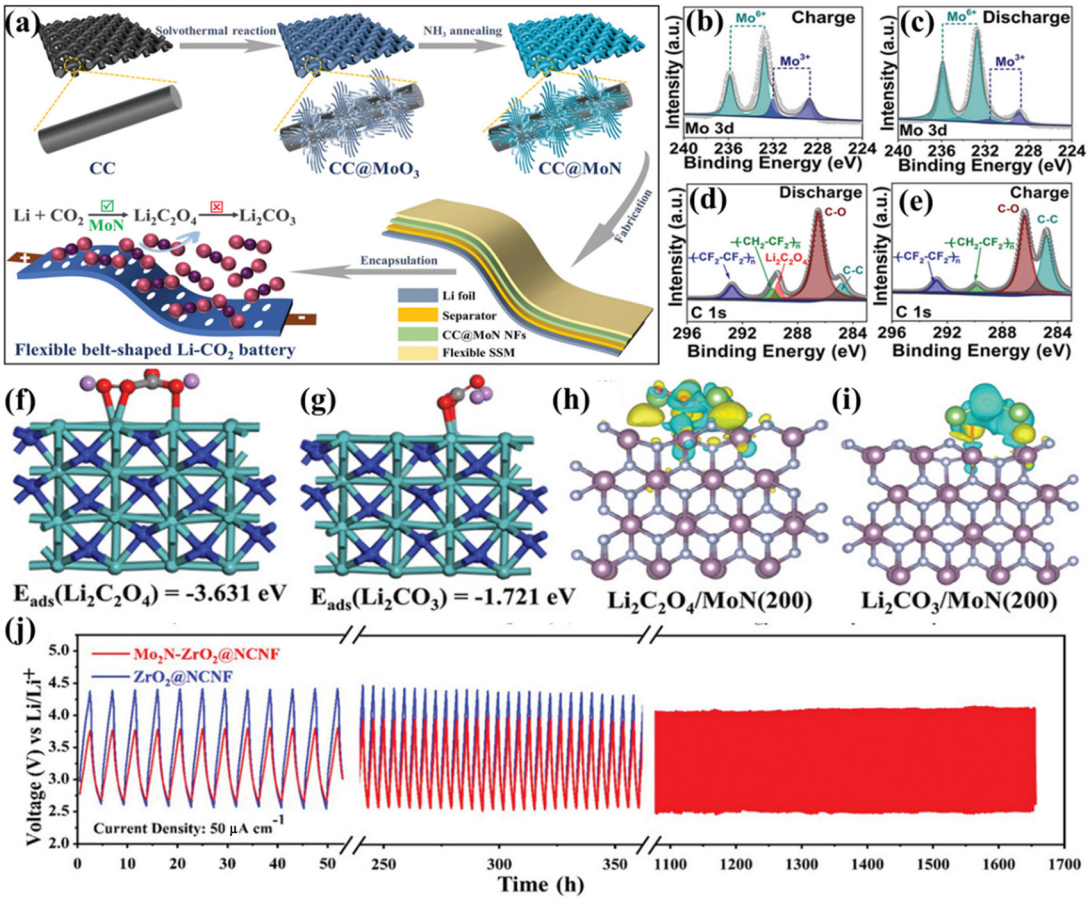

Fig. 13 (a) The diagram of the preparation process of binder-free freestanding CC@MoN NFs as flexible LCB cathodes. XPS spectra of (b and c) Mo 3d and (d and e) C 1s for CC@MoN NFs in the discharge and recharge states at 20 μA cm^{-2} with a capacity of 100 μAh cm^{-2}. (f and g) Side view of the optimized energy structure. (h and i) Charge density difference of $Li_2C_2O_4$ and Li_2CO_3 adsorbed on the MoN (200) surface.[102] Copyright 2021, Wiley-VCH GmbH. (j) The voltage/time curves of Mo_2N–ZrO_2@NCNFs at 50μA cm^{-2}.[103] Copyright 2023, Wiley-VCH GmbH.

in LCBs (Fig. 13a).[102] The researchers found through XPS and DFT calculations that the isolated Mo^{3+} ions in MoN were capable of stabilizing the 2-electron discharge intermediate $Li_2C_2O_4$, and a Mo–O coupling bridge was formed. This bridge facilitated the reversible production and decomposition of $Li_2C_2O_4$ (Fig. 13b–i). MoN exhibits ultra-high electronic conductivity and strong catalytic activity, but it has a weak interaction with CO_2, which decreases the efficiency of the battery. In contrast, the adsorption and conversion of CO_2 can be effectively enhanced with ZrO_2. Based on this, Cheng's group designed the MoN–ZrO_2 heterojunction material embedded on carbon nanofibers (CNFs) as a catalyst for LCBs.[103] The MoN–ZrO_2 heterostructure in the conductive CNF offers superior performance in accelerating electron transport, enhancing CO_2 conversion, and stabilizing the discharge product $Li_2C_2O_4$. Benefiting from these advantages, LCBs with Mo_2N–ZrO_2@NCNFs exhibit excellent cycling stability even at high current densities (Fig. 13j).

As a metalloid element, tellurium (Te) exhibits excellent electrical conductivity and strong CO_2 adsorption capabilities, and it shows potential in Li–CO_2 batteries.[72,104,105] Wang *et al.* constructed clusters of metal-like Te atoms anchored on N-doped carbon nanosheets (Te_{AC}@NCNSs) as cathode catalysts.[105] XPS analysis showed that C stabilized the Te atomic centers in the form of covalent bonds, and Te existed in the form of Te–O bonds (Fig. 14d). Te atom clusters were found to be the active centers, hindering the distribution of Li_2CO_3. This hindrance occurred due to the formation of Te–O bonds between Te and CO_3^{2-}. As a result, electron redistribution of the discharge product took place, leading to the formation of an amorphous thin film of Li_2CO_3 during the discharge process (Fig. 14b and c). This uniformly distributed thin-film Li_2CO_3 is easily decomposed by fully utilizing the abundant Te atom clusters, which greatly accelerates the decomposition of Li_2CO_3 (Fig. 14a).

Transition metal-based catalysts exhibit good catalytic activity in the field of electrocatalysis due to the presence of mostly lone-pair electrons of transition metal elements to form intermediates during chemical reactions and to reduce the reaction activation energy. However, agglomeration and detachment of metal particles tend to cause deactivation of transition metal-based catalysts, and their instability affects the battery life.

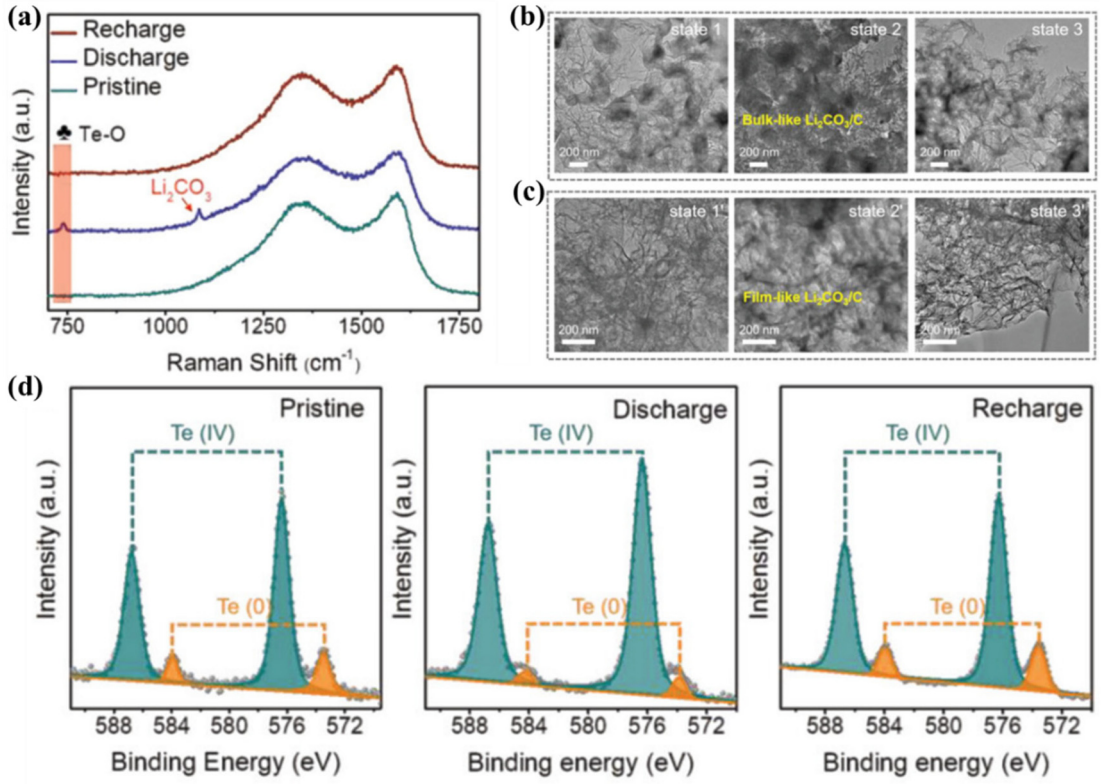

Fig. 14 (a) Raman spectra of the Te_{AC}@NCNS cathode in several states. TEM images of (b) NCNS and (c) Te_{AC}@NCNS cathodes in discharge and charge states. (d) The Te 3d XPS spectra of Te_{AC}@NCNS cathodes in pristine, discharge, and recharge states.[105] Copyright 2023, Wiley-VCH GmbH.

3.4 Metal/covalent organic frameworks (MOFs/COFs)

Both MOFs and COFs are crystalline porous materials that possess a large specific surface area, adjustable structure, and easy functionalization.[106,107] MOFs are crystalline porous materials first proposed by Yaghi *et al.* in 1995 by complexing metal ions with organic monomers.[108] In 2005, Yaghi *et al.* introduced the concept of COFs, which are a class of molecularly connected units made up of discrete organic molecules. These frameworks are formed through reversible covalent bonding, guided by reticular chemical interactions.[109] With high thermal and chemical stability, structural tunability and versatility, these porous materials have promising potential in areas of gas storage and adsorption and catalysis.[107,110,111] Wang's group investigated six different MOFs as multifunctional porous catalysts, which is the first time MOFs were introduced into the LCB system. They found that Mn(II)-centered MOFs significantly reduced the battery overpotential and improved the energy efficiency.[112] The advantages of MOFs in CO_2 utilization and reversible battery cycling allow them to be a new option for energy storage.

Recently, Zhang *et al.* reported a cathode catalyst of a covalent organic skeleton based on porphyrin (TTCOF-Mn) with a single metal site (Fig. 15a).[113] The assembled battery showed a potential of only 1.07 V at 100 mA g^{-1} and was stable for 180 reversible cycles at 300 mA g^{-1} (Fig. 15b and c). It has been determined by experimental and theoretical studies that the Mn-TAPP unit site in TTCOF-Mn exhibits a strong adsorption effect on CO_2. This allows for the efficient realization of the $4e^-$ non-protonic CO_2 conversion process. The discharge reaction occurring on the cathode of TTCOF-Mn can be represented using the equation: $4Li + 3CO_2 \rightarrow 2Li_2CO_3 + C$ (Fig. 15d–g). The catalytic active sites and reaction pathways of non-protonic LCBs were explored here for the first time. The diverse compositional and structural characteristics of porous crystalline-based materials make them highly applicable for electrochemical energy storage and catalytic applications.

Wang *et al.* designed a MOF-based photosensitive catalyst with phthalocyanine ligands of Co–N_4 and Mn ions.[38] Based on the design of the catalyst nanosheet morphology, more catalytically active sites were exposed. It makes the discharge products of the Co–Pc–Mn–O cathode in LCBs under light illumination show a nanosheet shape, while a rod shape for those without light illumination. Owing to the nanosheet morphology, the contact area between the active sites and the electrodes is increased, which improves the catalytic performance and accelerates the rapid decomposition of the discharge products. Zhao *et al.* proposed a bicontinuous hierarchical porous structure that combines the cathode material and solid polymer electrolyte,[43] which connects the mass transfer process pathway in the solid–solid–gas direction, improving the transport of lithium salts and CO_2. It is noteworthy that a plausible explanation is offered for the inactivation caused by the degradation of the battery capacity. The slowly decomposing Li_2CO_3 is difficult to reduce on a highly viscous polymer

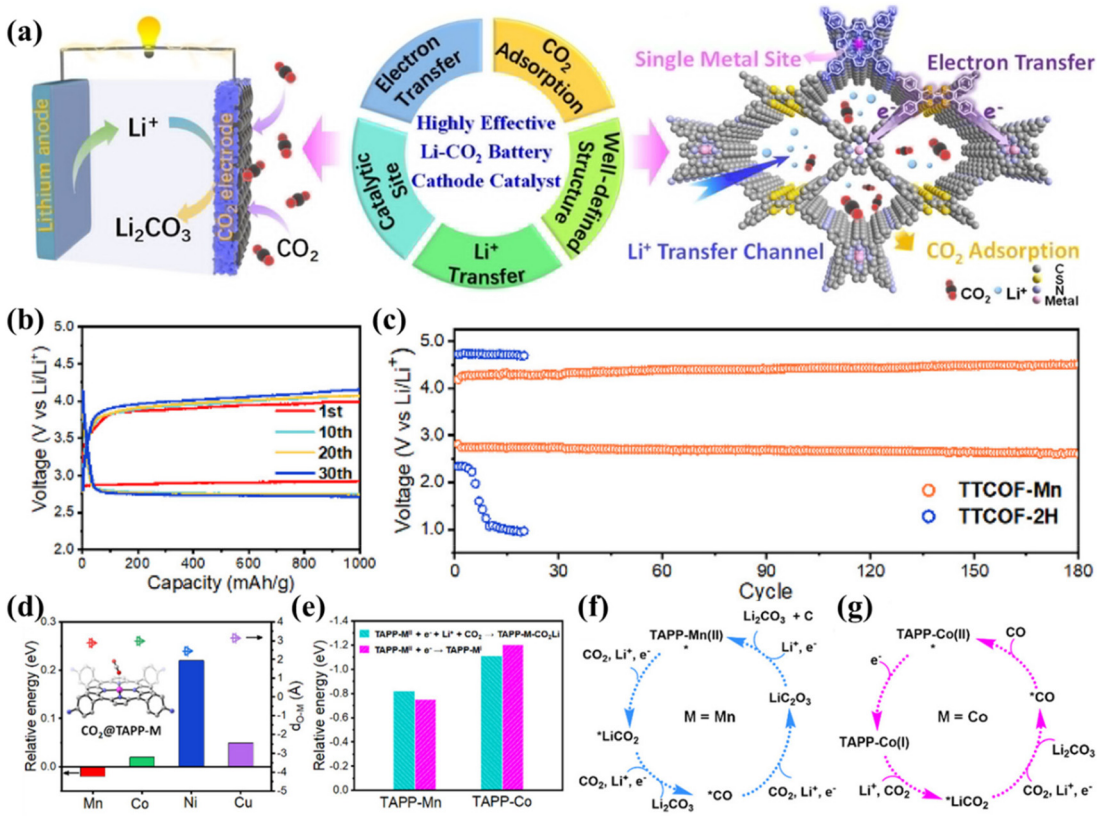

Fig. 15 (a) The descriptions of the advantages of TTCOF-M as a cathode catalyst for LCBs. (b) The discharge and charge curves of the TTCOF-Mn cathode at 100 mA g^{-1}. (c) The cycling curves of TTCOF-Mn and TTCOF-2H cathodes at 300 mA g^{-1}. (d) Energy curves for the adsorption of CO_2 on TAPP-M (M = Mn, Co, Ni, and Cu) molecules, with the corresponding molecules shown schematically in the inset. (e) The energy profiles of the first electron accepted by the TAPP-M (M = Mn and Co) molecule in two different pathways. (f) Schematic diagram of the four-electron pathway occurring at the TAPP-Mn site. (g) The diagram of the two-electron pathway occurring at the TAPP-Co site.[113] Copyright 2021, American Chemical Society.

electrolyte called "dead Li_2CO_3", which results in the deactivation of the battery by blocking ion transport. After the introduction of OM-ZIF-8, the polymer electrolyte remained smooth and intact, and the "dead Li_2CO_3" was removed by viscous flow. However solid polymer electrolytes have low room-temperature conductivity and the application of solid-state LCBs is limited to the temperature range.

Porous organic framework materials are characterized by their porous nature and large comparative area, and their structural and functional diversity, which makes them highly catalytically active. In contrast, the electrical conductivity of pure COF materials as catalysts for LCBs needs to be further improved, and the practical industrial applications of porous organic framework materials are very limited.

3.5 Molecular catalysts

The CRR/CER based on molecular catalysts attracts attention due to its high catalytic activity, well-defined active centers, and rational structural design.[114–116] Macrocyclic complexes with transition metal centers in molecular catalysts, either in solution (homogeneous catalysis) or anchored on carbon materials/electrodes (multiphase catalysis), have become effective catalysts for exploring CO_2 electroreduction reactions. In particular, metal porphyrins, phthalocyanines, and their derivatives have been widely studied.[117,118]

Zheng *et al.* reported a molecularly dispersed electrocatalyst (MDE) in which they catalyzed the reduction of CO_2 by dispersing nickel phthalocyanine (NiPc) over CNTs.[119] Moreover, the conductive network of CNT promotes CO_2 release, while the cyano-substituted material exhibits superior discharge performance and cycling stability compared to the mixture of NiPc and CNTs. A Li–CO_2 battery with the NiPc-CN MDE cathode material exhibits a polarization of only 1.4 V and stable operation for 120 cycles. Wu *et al.*[120] reported a novel 4,4′-bipyridine (BPD)-assisted LCB capable of reversible CO_2 capture/release (Fig. 16a). Studies found that BPD initially coordinates with two CO_2 molecules to form a [BPD···$2CO_2$] complex. The complex is then reduced through a two-electron pathway to give the discharge product Li_2[BPD–$2CO_2$]. Upon charging, Li_2[BPD–$2CO_2$] undergoes reversible oxidation, releasing BPD and CO_2 (Fig. 16b–e). The BPD cathode Li–CO_2 battery used as a proof-of-concept exhibited a high discharge capacity (>1000 mA h g^{-1}), a low polarization (0.3 V), and rare parasitic reactions. Wang *et al.* introduced a soluble redox

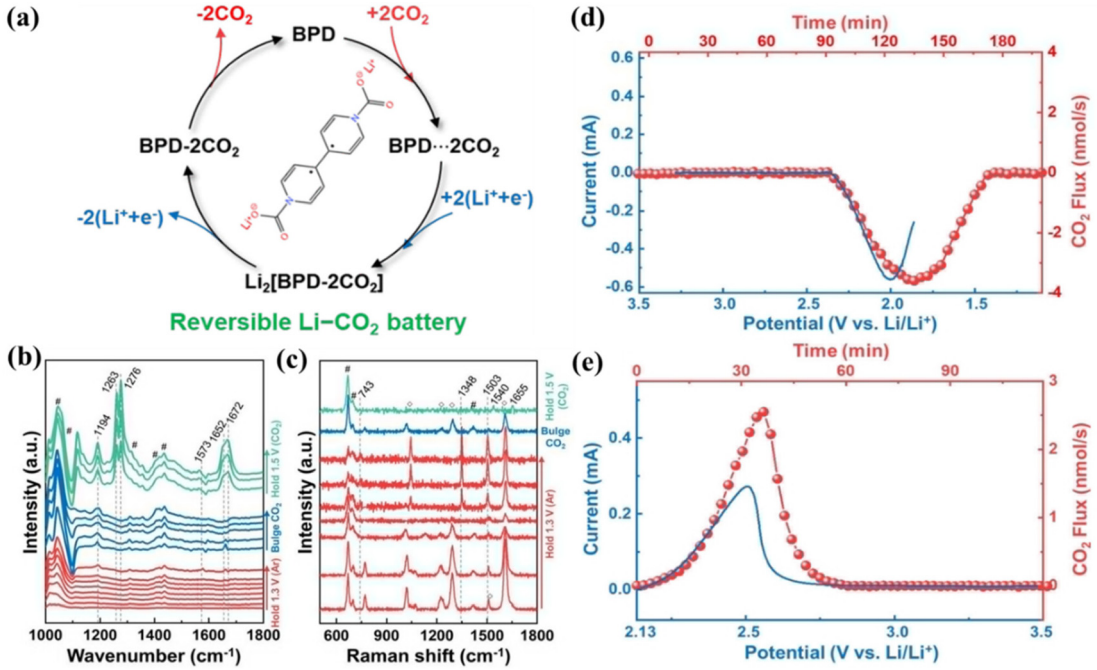

Fig. 16 (a) Schematic of the working mechanism of a BPD-assisted Li-CO_2 battery. (b) FT-IR spectra and GC results with an external reflection configuration. (c) SERS spectra recorded on Au for controlled electrochemical experimental conditions. The DEMS profile of a LCB during (d) cathodic and (e) anodic processes.[120] Copyright 2023, American Chemical Society.

mediator (2,2,6,6-tetramethylpiperidoxyl as the TEM RM) and reduced a graphene oxide electrode combined with CO_2 to form a "trinity" of LCBs.[121] The CRR process was mediated by TEM at potentials above 2.8 V, and CO_2 was selectively converted to $Li_2C_2O_4$. The TEM exhibited fast kinetics during charging, accelerating the rapid diffusion of Li^+ and facilitating the decomposition of the discharge products.

Conventional molecular catalysts are not very good at molecule-to-molecule conductivity and thus the current density is limited. Molecular catalysts are characterized by their tunable active sites, conductive substrates and customizable structure, which effectively improve the overall activity of catalysts.

Table 2 lists the representative research results achieved in recent years. The above research results show that the continuous development of catalysts for aprotic, photo-assisted, and all-solid-state LCBs has fueled their applications in energy conversion and storage.

Table 2 Summary of the recent progress in rechargeable LCBs with various catalysts. (* Represents mA g^{-1})

Cathode	Capacity/mA h g^{-1} (*)	Polarization/V (*)	Cycling stability/N (*)	Energy efficiency/%	Ref.
Graphene	6600 (100)	—	10 (100)	—	53
Carbon nanotubes	5786 (100)	—	22 (100)	—	54
VA-NCNTs	18 652 (100)	1.33 (50)	603 (500)	61	55
CQD/hG	12 300 (500)	1.02 (100)	235 (1000)	74.3	65
RuAC + SA@NCB	10 651.9 (100)	1.05 (100)	60 (300)	—	71
IrRu/N-CNTs	6228 (100)	—	600 (100)	—	72
IrO_2-N/CNTs	4634 (100)	1.34 (100)	316 (100)	—	73
RuO_2–TiO_2 NAs/CT	16 727 (250)	1.05 (250)	238 (250)	—	74
SA–Cu–NG	29 033 (100)	1.47 (1000)	538 (200)	—	87
Co-doped CeO_2/graphene aerogels	7860 (100)	1.53 (100)	100 (100)	—	91
Mn_2(dobdc)	18 022 (50)		50 (200)	—	112
TTCOF-Mn	13 018 (100)	1.07 (100)	180 (300)	—	113
NiPc-CN	18 000 (200)	1.39 (250)	120 (50)	—	119
CNT@C_3N_4	15.77 mA h cm^{-2} (0.1 mA cm^{-2})	0.04 (0.02 mA cm^{-2})	100 (0.1 mA cm^{-2})	86.1	14
TNAs@AgNPs	31.11 mA h cm^{-2} (0.1 mA cm^{-2})	0.3 (0.1 mA cm^{-2})	100 (0.1 mA cm^{-2})	86.9	13
SACr@NG/PCF	—	1.39 (100 μA cm^{-2})	350 (100 μA cm^{-2})	78	84
V-MoS_2/Co_9S_8	3954 μA h cm^{-2} (20 μA cm^{-2})	0.68 (20 μA cm^{-2})	63 (20 μA cm^{-2})	81.2	94
CC@MoN NFs	6542.9 μA h cm^{-2} (20 μA cm^{-2})	0.94 (100 μA cm^{-2})	86 (100 μA cm^{-2})	—	102
MoN–ZrO_2	5262.2 μA h cm^{-2} (20 μA cm^{-2})	1.89 (200 μA cm^{-2})	400 (500 μA cm^{-2})	—	103
TeAC@NCNSs	28.35 mA h cm^{-2} (0.05 mA cm^{-2})	0.97 (0.025 mA cm^{-2})	120 (0.1 mA cm^{-2})	76	105

4. Summary and outlook

The electrochemical conversion of CO_2 into high-value-added products is a promising solution to the global energy crisis and carbon emissions. Research on LCBs provides new insights into CO_2 capture and utilization. While LCBs are promising energy storage devices, there are still many difficulties and challenges to overcome in order to commercialize LCBs. The discharge product of LCBs is the solid insulator Li_2CO_3, which accumulates on the surface of the electrodes during the discharge process, leading to an increase in the internal resistance of the battery, a decrease in the efficiency of the energy conversion, and the creation of a large overpotential, which seriously affect the rechargeability and the cycling life of the battery and its commercial application. However, the reaction mechanism is not clear, the battery kinetics are slow, and the relationship between the catalyst and electrochemical performance is not clear; thus it remains a great challenge to realize the practical application of LCBs.[12] Currently, researchers are actively developing new high-efficiency cathode materials and catalysts to improve the CO_2 conversion efficiency, optimizing electrolytes, adjusting the battery system to improve the ionic conductivity and safety, and exploring the reaction mechanism of LCBs by combining knowledge from a variety of disciplines, including materials science and computational science, to further accelerate the commercialization of LCBs (Fig. 17).

Firstly, the efficiency of the catalyst plays a crucial role in determining the electrochemical performance of LCBs. Issues such as a large overpotential and limited reversibility constrain the development of batteries. Different catalysts with varying chemical structures can impact the diffusion of CO_2/Li^+ and the deposition of discharge products. Therefore, the connection between catalyst properties, electrochemical activity, and discharge product morphology requires further exploration. Currently, various methods such as heteroatom doping, strain engineering, and defect control are common for catalyst modification. Among them, monoatomic catalysts are one of the most promising materials due to their strong interactions between metal monoatoms and carriers, and their unique electronic structure that maximizes the use of active sites.[122] Moreover, high-entropy materials are also considered as promising catalyst materials for LCBs due to their complex multi-alloy structure, excellent chemical stability, surface electronic structure modulation ability, and resistance to metal deposition and electrolyte corrosion. Some nanostructured materials and organic porous materials including MOFs, COFs, and HOFs also have great potential in the application of LCBs. In the research and development of photocatalysts, the use of light-assisted hot electrons generated by the resonance of equipartitioned excitons on the catalyst surface and the effects of locally formed electromagnetic fields on the electrochemical performance of the battery raise potential options for improving the energy efficiency. Additionally, the reaction process of the photocatalyst in the battery and the side reactions it induces are issues that need to be considered. A deeper understanding of catalyst properties is imperative for the design and development of efficient LCBs.

Secondly, a more comprehensive study of the reaction mechanism is necessary for the development of high-energy-density LCBs. Due to the unclear mechanism, it is difficult to fully explain the role of catalysts in the battery cycling process and to rationally design catalysts for constructing LCBs with high selectivity and activity. While some non-*in situ* characterization methods can assess the state at various stages of the reaction, obtaining a more profound and precise understand-

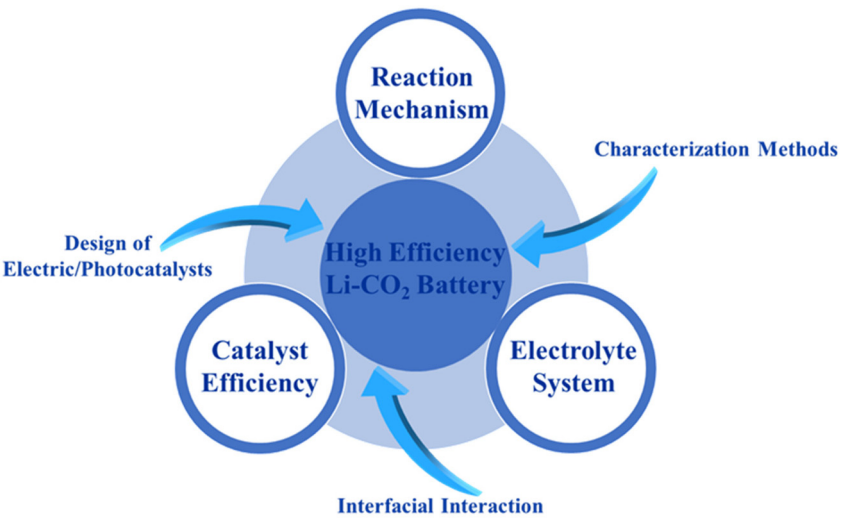

Fig. 17 Schematic illustration of the challenges faced by Li-CO_2 batteries and the corresponding solutions.

ing of the battery's charging and discharging processes remains challenging. Therefore, it is important to provide a more rigorous explanation of specific reaction mechanisms through various advanced quantitative and qualitative analysis techniques.

Thirdly, as LCBs are open systems, the stability of the multiphase interface is fundamental for the long cycle life of the battery. The development of solid-state electrolytes is an ideal method to alleviate the problems of electrolyte volatilization and leakage and to facilitate the development of wearable flexible batteries. Currently, lithium-ion conductivity, a wider electrochemical window, and electrochemical stabilization are important parameters explored for LCBs. The design and selection of solid-state electrolyte materials need to consider the interactions at the electrolyte/electrode interface. The passivation problem of the cathode is very prominent in both liquid and solid-state LCBs, and the design of an efficient catalyst is essential. It is worth noting that current techniques for characterizing all-solid-state LCBs are not comprehensive enough, and electrochemical *in situ* characterization methods for observing the dynamics of the battery during operation are a worthwhile approach to consider.

In summary, LCBs represent an innovative technology for energy storage and conversion, but many challenges remain to be overcome for practical applications. Clarifying the working mechanism, understanding the nature of the catalyst, and designing and developing a highly stable electrolyte are crucial for achieving efficient LCBs.

Data availability

Data availability is not applicable to this article as no new data were created or analyzed in this study.

Conflicts of interest

There are no conflicts to declare.

Acknowledgements

The authors acknowledge the financial support for this work from the Fund Project for the National Defense Technology Innovation Special Zone Spark Project (2016300TS00911901), a Project Funded by the Priority Academic Program Development of Jiangsu Higher Education Institutions (PAPD), the Postgraduate Research & Practice Innovation Program of NUAA (xcxjh20230608 and xcxjh20230614), and the Project of Zhongyuan Critical Metals Laboratory (GJJSGFYQ202422).

References

1 C. Mora, D. Spirandelli, E. C. Franklin, J. Lynham, M. B. Kantar, W. Miles, C. Z. Smith, K. Freel, J. Moy, L. V. Louis, E. W. Barba, K. Bettinger, A. G. Frazier, J. F. Colburn IX, N. Hanasaki, E. Hawkins, Y. Hirabayashi, W. Knorr, C. M. Little, K. Emanuel, J. Sheffield, J. A. Patz and C. L. Hunter, Broad threat to humanity from cumulative climate hazards intensified by greenhouse gas emissions, *Nat. Clim. Change*, 2018, **8**, 1062–1071.

2 S. A. Montzka, E. J. Dlugokencky and J. H. Butler, Non-CO_2 greenhouse gases and climate change, *Nature*, 2011, **476**, 43–50.

3 M. G. Kibria, C. Dinh, A. Seifitokaldani, P. De Luna, T. Burdyny, R. Quintero-Bermudez, M. B. Ross, O. S. Bushuyev, F. P. García de Arquer, P. Yang, D. Sinton and E. H. Sargent, A Surface Reconstruction Route to High Productivity and Selectivity in CO_2 Electroreduction toward C_{2+} Hydrocarbons, *Adv. Mater.*, 2018, **30**, 1804867.

4 J. Du, Y. Han, H. Zhang, X. Gao, J. Guan and A. Chen, CoP_2O_6-Assisted Copper/Carbon Catalyst for Electrocatalytic Reduction of CO_2 to Formate, *ACS Nano*, 2023, **17**, 10055–10064.

5 X. Yang, X. Li, M. Liu, S. Yang, Q. Niu, L. Zhai, Z. Jiang, Q. Xu and G. Zeng, Modulating Electrochemical CO_2 Reduction Performance via Sulfur-Containing Linkages Engineering in Metallophthalocyanine Based Covalent Organic Frameworks, *ACS Mater. Lett.*, 2023, **5**, 1611–1618.

6 P. G. Bruce, S. A. Freunberger, L. J. Hardwick and J. M. Tarascon, Li-O_2 and Li-S batteries with high energy storage, *Nat. Mater.*, 2012, **11**, 19–29.

7 K. Takechi, T. Shiga and T. Asaoka, A Li-O_2/CO_2 battery, *Chem. Commun.*, 2011, **47**, 3463–3465.

8 T. Wei, X. Liu, S. Yang, P. Wang and T. Yi, Regulating the electrochemical activity of Fe-Mn-Cu-based layer oxides as cathode materials for high-performance Na-ion battery, *J. Energy Chem.*, 2023, **80**, 603–613.

9 T. Wei, P. Peng, Y. Ji, Y. Zhu, T. Yi and Y. Xie, Rational construction and decoration of $Li_5Cr_7Ti_6O_{25}$@C nanofibers as stable lithium storage materials, *J. Energy Chem.*, 2022, **71**, 400–410.

10 H. Chang, X. Liu, S. Zhao, Z. Liu, R. Lv, Q. Zhang and T. Yi, Self-Assembled 3D N/P/S-Tridoped Carbon Nanoflowerwith Highly Branched Carbon Nanotubes as Efficient Bifunctional Oxygen Electrocatalyst Toward High-Performance Rechargeable Zn-Air Batteries, *Adv. Funct. Mater.*, 2024, **34**, 2313491.

11 W. Liu, X. Sui, C. Cai, H. Huang, R. Xu, D. Geng, M. Chen and J. Lu, A Nonaqueous Mg-CO_2 Battery with Low Overpotential, *Adv. Energy Mater.*, 2022, **12**, 2201675.

12 X. Mu, H. Pan, P. He and H. Zhou, Li-CO_2 and Na-CO_2 Batteries: Toward Greener and Sustainable Electrical Energy Storage, *Adv. Mater.*, 2020, **32**, 1903790.

13 K. Zhang, J. Li, W. Zhai, C. Li, Z. Zhu, X. Kang, M. Liao, L. Ye, T. Kong, C. Wang, Y. Zhao, P. Chen, Y. Gao, B. Wang and H. Peng, Boosting Cycling Stability and Rate Capability of Li-CO_2 Batteries via Synergistic Photoelectric Effect and Plasmonic Interaction, *Angew. Chem., Int. Ed.*, 2022, **61**, e202201718.

14 J. Li, K. Zhang, Y. Zhao, C. Wang, L. Wang, L. Wang, M. Liao, L. Ye, Y. Zhang, Y. Gao, B. Wang and H. Peng, High-Efficiency and Stable Li-CO_2 Battery Enabled by Carbon Nanotube/Carbon Nitride Heterostructured Photocathode, *Angew. Chem., Int. Ed.*, 2022, **61**, e202114612.
15 D. Na, R. K. Kampara, D. Yu, B. Yoon, S. W. Martin and I. Seo, $Li_{1.4}Al_{0.4}Ti_{1.6}(PO_4)_3$ inorganic solid electrolyte for all-solid-state Li-CO_2 batteries with MWCNT and Ru nanoparticle catalysts, *Mater. Today Energy*, 2023, **38**, 101418.
16 D. Guan, X. Wang, F. Li, L. Zheng, M. Li, H. Wang and J. Xu, All-Solid-State Photo-Assisted Li-CO_2 Battery Working at an Ultra-Wide Operation Temperature, *ACS Nano*, 2022, **16**, 12364–12376.
17 S. Wang, H. Song, T. Zhu, J. Chen, Z. Yu, P. Wang, L. Yu, J. Xu, H. Zhou and K. Chen, An ultralow-charge-overpotential and long-cycle-life solid-state Li-CO_2 battery enabled by plasmon-enhanced solar photothermal catalysis, *Nano Energy*, 2022, **100**, 107521.
18 Y. Jiao, J. Qin, H. M. K. Sari, D. Li, X. Li and X. Sun, Recent progress and prospects of Li-CO_2 batteries: Mechanisms, catalysts and electrolytes, *Energy Storage Mater.*, 2021, **34**, 148–170.
19 Y. Xu, Y. Xia, H. Xue, H. Gong, K. Chang, J. He, T. Wang and R. Ma, Aprotic Lithium-Carbon Dioxide Batteries: Reaction Mechanism and Catalyst Design, *Chem. Rec.*, 2022, **22**, e202200109.
20 S. Xu, S. K. Das and L. A. Archer, The Li-CO_2 battery: a novel method for CO_2 capture and utilization, *RSC Adv.*, 2013, **3**, 6656–6660.
21 Y. Liu, R. Wang, Y. Lyu, H. Li and L. Chen, Rechargeable Li/CO_2-O_2 (2 : 1) battery and Li/CO_2 battery, *Energy Environ. Sci.*, 2014, **7**, 677–681.
22 Y. Qiao, J. Yi, S. Wu, Y. Liu, S. Yang, P. He and H. Zhou, Li-CO_2 Electrochemistry: A New Strategy for CO_2 Fixation and Energy Storage, *Joule*, 2017, **1**, 359–370.
23 S. Yang, P. He and H. Zhou, Exploring the electrochemical reaction mechanism of carbonate oxidation in Li-air/CO_2 battery through tracing missing oxygen, *Energy Environ. Sci.*, 2016, **9**, 1650–1654.
24 N. Mahne, S. E. Renfrew, B. D. McCloskey and S. A. Freunberger, Electrochemical Oxidation of Lithium Carbonate Generates Singlet Oxygen, *Angew. Chem., Int. Ed.*, 2018, **57**, 5529–5533.
25 Q. He, J. H. Lee, D. Liu, Y. Liu, Z. Lin, Z. Xie, S. Hwang, S. Kattel, L. Song and J. G. Chen, Accelerating CO_2 Electroreduction to CO Over Pd Single-Atom Catalyst, *Adv. Funct. Mater.*, 2020, **30**, 2000407.
26 Q. Wang, K. Liu, K. Hu, C. Cai, H. Li, H. Li, M. Herran, Y. Lu, T. Chan, C. Ma, J. Fu, S. Zhang, Y. Liang, E. Cortés and M. Liu, Attenuating metal-substrate conjugation in atomically dispersed nickel catalysts for electroreduction of CO_2 to CO, *Nat. Commun.*, 2022, **13**, 6082.
27 P. Ho, S. Cheng, F. Yu, Y. Yeung, W. Ni, C. Ko, C. Leung, T. Lau and M. Robert, Light-Driven Reduction of CO_2 to CO in Water with a Cobalt Molecular Catalyst and an Organic Sensitizer, *ACS Catal.*, 2023, **13**, 5979–5985.
28 J. Xie, Q. Liu, Y. Huang, M. Wu and Y. Wang, A porous Zn cathode for Li-CO_2 batteries generating fuel-gas CO, *J. Mater. Chem. A*, 2018, **6**, 13952–13958.
29 W. Ma, S. Xie, X. Zhang, F. Sun, J. Kang, Z. Jiang, Q. Zhang, D. Wu and Y. Wang, Promoting electrocatalytic CO_2 reduction to formate via sulfur-boosting water activation on indium surfaces, *Nat. Commun.*, 2019, **10**, 892.
30 X. Zheng, P. De Luna, F. P. García De Arquer, B. Zhang, N. Becknell, M. B. Ross, Y. Li, M. N. Banis, Y. Li, M. Liu, O. Voznyy, C. T. Dinh, T. Zhuang, P. Stadler, Y. Cui, X. Du, P. Yang and E. H. Sargent, Promoting electrocatalytic CO_2 reduction to formate via sulfur-boosting water activation on indium surfaces, *Joule*, 2017, **1**, 794–805.
31 W. He, J. Xiong, Z. Tang, Y. Wang, X. Wang, H. Xu, Z. Zhao, J. Liu and Y. Wei, Localized surface plasmon resonance effect of bismuth nanoparticles in Bi/TiO_2 catalysts for boosting visible light-driven CO_2 reduction to CH_4, *Appl. Catal., B*, 2024, **344**, 123651.
32 X. Liang, Q. Zheng, N. Wei, Y. Lou, S. Hu, K. Zhao, H. Liao, N. Tian, Z. Zhou and S. Sun, *In situ* constructing Bi@$Bi_2O_2CO_3$ nanosheet catalyst for ampere-level CO_2 electroreduction to formate, *Nano Energy*, 2023, **114**, 108638.
33 H. Xue, H. Gong, X. Lu, B. Gao, T. Wang, J. He, Y. Yamauchi, T. Sasaki and R. Ma, Aqueous Formate-Based Li-CO_2 Battery with Low Charge Overpotential and High Working Voltage, *Adv. Energy Mater.*, 2021, **11**, 2101630.
34 Y. Hou, J. Wang, L. Liu, Y. Liu, S. Chou, D. Shi, H. Liu, Y. Wu, W. Zhang and J. Chen, Mo_2 C/CNT: An Efficient Catalyst for Rechargeable Li-CO_2 Batteries, *Adv. Funct. Mater.*, 2017, **27**, 1700564.
35 J. Zhou, X. Li, C. Yang, Y. Li, K. Guo, J. Cheng, D. Yuan, C. Song, J. Lu and B. Wang, A Quasi-Solid-State Flexible Fiber-Shaped Li-CO_2 Battery with Low Overpotential and High Energy Efficiency, *Adv. Mater.*, 2019, **31**, 1804439.
36 X. Sun, X. Mu, W. Zheng, L. Wang, S. Yang, C. Sheng, H. Pan, W. Li, C. Li, P. He and H. Zhou, Binuclear Cu complex catalysis enabling Li-CO_2 battery with a high discharge voltage above 3.0 V, *Nat. Commun.*, 2023, **14**, 536.
37 X. Yang, X. Lan, Y. Zhang, H. Li and G. Bai, Rational design of MoS_2@COF hybrid composites promoting C-C coupling for photocatalytic CO_2 reduction to ethane, *Appl. Catal., B*, 2023, **325**, 122393.
38 J. Wang, S. Li, Y. Chen, L. Dong, M. Liu, J. Shi, S. Li and Y. Lan, Phthalocyanine Based Metal-Organic Framework Ultrathin Nanosheet for Efficient Photocathode toward Light-Assisted Li-CO_2 Battery, *Adv. Funct. Mater.*, 2022, **32**, 2210259.
39 X. Yu, G. Liu, T. Wang, H. Gong, H. Qu, X. Meng, J. He and J. Ye, Recent Advances in the Research of Photo-Assisted Lithium-Based Rechargeable Batteries, *Chem. – Eur. J.*, 2022, **28**, e202202104.
40 Z. Zhu, X. Shi, G. Fan, F. Li and J. Chen, Photo-energy Conversion and Storage in an Aprotic Li-O_2 Battery, *Angew. Chem.*, 2019, **131**, 19197–19202.

41 D. Li, X. Lang, Y. Guo, Y. Wang, Y. Wang, H. Shi, S. Wu, W. Wang and Q. Yang, A photo-assisted electrocatalyst coupled with superoxide suppression for high performance Li-O_2 batteries, *Nano Energy*, 2021, **85**, 105966.
42 D. Guan, X. Wang, M. Li, F. Li, L. Zheng, X. Huang and J. Xu, Light/Electricity Energy Conversion and Storage for a Hierarchical Porous In_2S_3@CNT/SS Cathode towards a Flexible Li-CO_2 Battery, *Angew. Chem., Int. Ed.*, 2020, **59**, 19518–19524.
43 J. Zhao, Y. Wang, H. Zhao, L. Liu, S. Li, X. Hu and S. Ding, Enabling All-Solid-State Lithium-Carbon Dioxide Battery Operation in a Wide Temperature Range, *ACS Nano*, 2024, **18**, 5132–5140.
44 R. Wang, X. Zhang, Y. Cai, Q. Nian, Z. Tao and J. Chen, Safety-reinforced rechargeable Li-CO2 battery based on a composite solid state electrolyte, *Nano Res.*, 2019, **12**, 2543–2548.
45 T. Yang, H. Li, J. Chen, H. Ye, J. Yao, Y. Su, B. Guo, Z. Peng, T. Shen, Y. Tang, L. Zhang and J. Huang, In situ imaging electrocatalytic CO_2 reduction and evolution reactions in all-solid-state Li-CO_2 nanobatteries, *Nanoscale*, 2020, **12**, 23967–23974.
46 Y. Guo, S. Wu, Y. He, F. Kang, L. Chen, H. Li and Q. Yang, Solid-state lithium batteries: Safety and prospects, *eScience*, 2022, **2**, 138–163.
47 J. Chang, Q. Huang and Z. Zheng, A Figure of Merit for Flexible Batteries, *Joule*, 2020, **4**, 1346–1349.
48 Q. Zhai, F. Xiang, F. Cheng, Y. Sun, X. Yang, W. Lu and L. Dai, Recent advances in flexible/stretchable batteries and integrated devices, *Energy Storage Mater.*, 2020, **33**, 116–138.
49 M. Mushtaq, X. Guo, J. Bi, Z. Wang and H. Yu, Polymer electrolyte with composite cathode for solid-state Li-CO_2 battery, *Rare Met.*, 2018, **37**, 520–526.
50 D. D. Tune, B. S. Flavel, R. Krupke and J. G. Shapter, Carbon Nanotube-Silicon Solar Cells, *Adv. Energy Mater.*, 2012, **2**, 1043–1055.
51 F. Ye, L. Gong, Y. Long, S. Talapaneni, L. Zhang, Y. Xiao, D. Liu, C. Hu and L. Dai, Topological Defect-Rich Carbon as a Metal-Free Cathode Catalyst for High-Performance Li-CO_2 Batteries, *Adv. Energy Mater.*, 2021, **11**, 2101390.
52 Y. Xiao, F. Du, C. Hu, Y. Ding, Z. Wang, A. Roy and L. Da, High-Performance Li-CO_2 Batteries from Free-Standing, Binder-Free, Bifunctional Three-Dimensional Carbon Catalysts, *ACS Energy Lett.*, 2020, **5**, 916–921.
53 Z. Zhang, Q. Zhang, Y. Chen, J. Bao, X. Zhou, Z. Xie, J. Wei and Z. Zhou, The First Introduction of Graphene to Rechargeable Li-CO_2 Batteries, *Angew. Chem., Int. Ed.*, 2015, **54**, 6550–6553.
54 X. Zhang, Q. Zhang, Z. Zhang, Y. Chen, Z. Xie, J. Wei and Z. Zhou, Rechargeable Li-CO_2 batteries with carbon nanotubes as air cathodes, *Chem. Commun.*, 2015, **51**, 14636–14639.
55 X. Li, J. Zhang, G. Qi, J. Cheng and B. Wang, Vertically Aligned N-doped Carbon Nanotubes Arrays as Efficient Binder-free Catalysts for Flexible Li-CO_2 Batteries, *Energy Storage Mater.*, 2021, **35**, 148–156.
56 W. Yu, L. Liu, Y. Yang, N. Li, Y. Chen, X. Yin, J. Niu, J. Wang and S. Ding, N, O-diatomic dopants activate catalytic activity of 3D self-standing graphene carbon aerogel for long-cycle and high-efficiency Li-CO_2 batteries, *Chem. Eng. J.*, 2023, **465**, 142787.
57 Z. Sun, D. Wang, L. Lin, Y. Liu, M. Yuan, C. Nan, H. Li, G. Sun and X. Yang, Ultrathin hexagonal boron nitride as a van der Waals' force initiator activated graphene for engineering efficient non-metal electrocatalysts of Li-CO_2 battery, *Nano Res.*, 2022, **15**, 1171.
58 F. Xiao, Z. Lin, J. Zhang, Y. Lei, Y. Meng, X. Chen, S. Zhao, B. Hong, J. Wang, D. Li and J. Xu, A novel approach to facile synthesis of boron and nitrogen co-doped graphene and its application in lithium oxygen batteries, *Energy Storage Mater.*, 2021, **41**, 61–68.
59 S. Chen, Z. Chen, S. Siahrostami, D. Higgins, D. Nordlund, D. Sokaras, T. R. Kim, Y. Liu, X. Yan, E. Nilsson, R. Sinclair, J. K. Nørskov, T. F. Jaramillo and Z. Bao, Designing Boron Nitride Islands in Carbon Materials for Efficient Electrochemical Synthesis of Hydrogen Peroxide, *J. Am. Chem. Soc.*, 2018, **140**, 7851–7859.
60 X. Li, B. Lin, H. Li, Q. Yu, Y. Ge, X. Jin, X. Liu, Y. Zhou and J. Xiao, Carbon doped hexagonal BN as a highly efficient metal-free base catalyst for Knoevenagel condensation reaction, *Appl. Catal., B*, 2018, **239**, 254–259.
61 A. S. Varela, W. Ju and P. Strasser, Molecular Nitrogen-Carbon Catalysts, Solid Metal Organic Framework Catalysts, and Solid Metal/Nitrogen-Doped Carbon (MNC) Catalysts for the Electrochemical CO_2 Reduction, *Adv. Energy Mater.*, 2018, **8**, 1703614.
62 Z. Xu, S. Lin, N. Onofrio, L. Zhou, F. Shi, W. Lu, K. Kang, Q. Zhang and S. P. Lau, Exceptional catalytic effects of black phosphorus quantum dots in shuttling-free lithium sulfur batteries, *Nat. Commun.*, 2018, **9**, 4164.
63 M. H. Elsayed, J. Jayakumar, M. Abdellah, T. H. Mansoure, K. Zheng, A. M. Elewa, C. Chang, L. Ting, W. Lin, H. Yu, W. Wang, C. Chung and H. Chou, Visible-light-driven hydrogen evolution using nitrogen-doped carbon quantum dot-implanted polymer dots as metal-free photocatalysts, *Appl. Catal., B*, 2021, **283**, 119659.
64 M. F. Kuehnel, K. L. Orchard, K. E. Dalle and E. Reisner, Selective Photocatalytic CO_2 Reduction in Water through Anchoring of a Molecular Ni Catalyst on CdS Nanocrystals, *J. Am. Chem. Soc.*, 2017, **139**, 7217–7223.
65 Y. Jin, C. Hu, Q. Dai, Y. Xiao, Y. Lin, J. W. Connell, F. Chen and L. Dai, High-Performance Li-CO_2 Batteries Based on Metal-Free Carbon Quantum Dot/Holey Graphene Composite Catalysts, *Adv. Funct. Mater.*, 2018, **28**, 1804630.
66 X. Hu, Z. Li and J. Chen, Flexible Li-CO_2 Batteries with Liquid-Free Electrolyte, *Angew. Chem., Int. Ed.*, 2017, **56**, 5785–5789.
67 X. Cao, C. Wei, X. Zheng, K. Zeng, X. Chen, M. H. Rummeli, P. Strasser and R. Yang, Ru clusters

anchored on Magnéli phase Ti_4O_7 nanofibers enables flexible and highly efficient Li-O_2 batteries, *Energy Storage Mater.*, 2022, **50**, 355–364.

68 Y. Zhu, K. Fan, C. Hsu, G. Chen, C. Chen, T. Liu, Z. Lin, S. She, L. Li, H. Zhou, Y. Zhu, H. M. Chen and H. Huang, Supported Ruthenium Single-Atom and Clustered Catalysts Outperform Benchmark Pt for Alkaline Hydrogen Evolution, *Adv. Mater.*, 2023, **35**, 2301133.

69 K. Baek, W. C. Jeon, S. Woo, J. C. Kim, J. G. Lee, K. An, S. K. Kwak and S. J. Kang, Synergistic effect of quinary molten salts and ruthenium catalyst for high-power-density lithium-carbon dioxide cell, *Nat. Commun.*, 2020, **11**, 456.

70 S. Yang, Y. Qiao, P. He, Y. Liu, Z. Cheng, J. Zhu and H. Zhou, A reversible lithium-CO_2 battery with Ru nanoparticles as a cathode catalyst, *Energy Environ. Sci.*, 2017, **10**, 972–978.

71 J. Lin, J. Ding, H. Wang, X. Yang, X. Zheng, Z. Huang, W. Song, J. Ding, X. Han and W. Hu, Boosting Energy Efficiency and Stability of Li–CO_2 Batteries via Synergy between Ru Atom Clusters and Single-Atom Ru–N4 sites in the Electrocatalyst Cathode, *Adv. Mater.*, 2022, **34**, 2200559.

72 Z. Wang, B. Liu, X. Yang, C. Zhao, P. Dong, X. Li, Y. Zhang, K. Doyle-Davis, X. Zeng, Y. Zhang and X. Sun, Dual Catalytic Sites of Alloying Effect Bloom CO_2 Catalytic Conversion for Highly Stable Li-CO_2 Battery, *Adv. Funct. Mater.*, 2023, **33**, 2213931.

73 G. Wu, X. Li, Z. Zhang, P. Dong, M. Xu, H. Peng, X. Zeng, Y. Zhang and S. Liao, Design of ultralong-life Li-CO_2 batteries with IrO_2 nanoparticles highly dispersed on nitrogen-doped carbon nanotubes, *J. Mater. Chem. A*, 2020, **8**, 3763–3770.

74 C. Wang, Y. Shang, Y. Lu, L. Qu, H. Yao, Z. Li and Q. Liu, Photoinduced homogeneous RuO_2 nanoparticles on TiO_2 nanowire arrays: A high-performance cathode toward flexible Li-CO_2 batteries, *J. Power Sources*, 2020, **475**, 228703.

75 K. V. Savunthari, C. Chen, Y. Chen, Z. Tong, K. Iputera, F. Wang, C. Hsu, D. Wei, S. Hu and R. Liu, Effective Ru/CNT Cathode for Rechargeable Solid-State Li-CO_2 Batteries, *ACS Appl. Mater. Interfaces*, 2021, **13**, 44266–44273.

76 J. Li, K. Zhang, B. Wang and H. Peng, Light-Assisted Metal-Air Batteries: Progress, Challenges, and Perspectives, *Angew. Chem., Int. Ed.*, 2022, **61**, e202213026.

77 S. Jiang, S. Yang, W. Huang, H. Sung, R. Lin, J. Li, B. Tsai, T. Agnihotri, Y. Nikodimos, C. Wang, S. D. Lin, C. Wang, S. Wu, W. Su and B. J. Hwang, Enhancing the interfacial stability between argyrodite sulfide-based solid electrolytes and lithium electrodes through CO_2 adsorption, *J. Mater. Chem. A*, 2023, **11**, 2910–2919.

78 Y. Du, Y. Liu, S. Yang, C. Li, Z. Cheng, F. Qiu, P. He and H. Zhou, A rechargeable all-solid-state Li-CO_2 battery using a $Li_{1.5}Al_{0.5}Ge_{1.5}(PO_4)_3$ ceramic electrolyte and nanoscale RuO_2 catalyst, *J. Mater. Chem. A*, 2021, **9**, 9581–9585.

79 S. Wang, B. Li, L. Li, Z. Tian, Q. Zhang, L. Chen and X. C. Zeng, Highly efficient N_2 fixation catalysts: transition-metal carbides M_2C(MXenes), *Nanoscale*, 2020, **12**, 538–547.

80 C. M. Tseng, C. Huang, J. Pai and Y. Li, Co Single Atom-FeCo Alloy-Carbon Nanotube Catalysts on Graphene for Lithium-Oxygen and Lithium-Carbon Dioxide Batteries, *ACS Sustainable Chem. Eng.*, 2023, **11**, 8120–8130.

81 Y. Xu, H. Gong, L. Song, Y. Kong, C. Jiang, H. Xue, P. Li, X. Huang, J. He and T. Wang, A highly efficient and free-standing copper single atoms anchored nitrogen-doped carbon nanofiber cathode toward reliable Li-CO_2 batteries, *Mater. Today Energy*, 2022, **25**, 100967.

82 S. Yin, J. Zhao, S. Wu, X. Wang, Y. Quan and J. Ren, Electrochemical reduction of CO_2 to CO on bimetallic CoCu-N-C catalyst, *J. Cleaner Prod.*, 2022, **371**, 133569.

83 C. Wang, H. Ren, Z. Wang, Q. Guan, Y. Liu and W. Li, A promising single-atom Co-N-C catalyst for efficient CO_2 electroreduction and high-current solar conversion of CO_2 to CO, *Appl. Catal., B*, 2022, **304**, 120958.

84 Y. Liu, S. Zhao, D. Wang, B. Chen, Z. Zhang, J. Sheng, X. Zhong, X. Zou, S. P. Jiang, G. Zhou and H. Cheng, Toward an Understanding of the Reversible Li-CO_2 Batteries over Metal-N_4-Functionalized Graphene Electrocatalysts, *ACS Nano*, 2022, **16**, 1523–1532.

85 E. Zhang, T. Wang, K. Yu, J. Liu, W. Chen, A. Li, H. Rong, R. Lin, S. Ji, X. Zheng, Y. Wang, L. Zheng, C. Chen, D. Wang, J. Zhang and Y. Li, Bismuth Single Atoms Resulting from Transformation of Metal-Organic Frameworks and Their Use as Electrocatalysts for CO_2 Reduction, *J. Am. Chem. Soc.*, 2019, **141**, 16569–16573.

86 H. Wong, T. Liu, M. Tamtaji, X. Huang, T. W. Tang, M. D. Hossain, J. Wang, Y. Cai, Z. Liu, H. Liu, K. Amine, W. A. Goddard and Z. Luo, Graphene-supported single atom catalysts for high performance lithium-oxygen batteries, *Nano Energy*, 2024, **121**, 109279.

87 Y. Xu, X. Li, Y. Li, Y. Wang, L. Song, J. Ding, X. Fan, J. He, T. Wang and Z. Wu, Reconfiguration of the charge density difference of nitrogen-doped graphene by covalently bonded Cu-N_4 active sites boosting thermodynamics and performance in aprotic Li-CO_2 battery, *Energy Storage Mater.*, 2024, **68**, 103354.

88 J. Wang, S. Kim, J. Liu, Y. Gao, S. Choi, J. Han, H. Shin, S. Jo, J. Kim, F. Ciucci, H. Kim, Q. Li, W. Yang, X. Long, S. Yang, S.-P. Cho, K. H. Chae, M. G. Kim, H. Kim and J. Lim, Redirecting dynamic surface restructuring of a layered transition metal oxide catalyst for superior water oxidation, *Nat. Catal.*, 2021, **4**, 212–222.

89 X. Long, H. Lin, D. Zhou, Y. An and S. Yang, Enhancing Full Water-Splitting Performance of Transition Metal Bifunctional Electrocatalysts in Alkaline Solutions by Tailoring CeO_2-Transition Metal Oxides-Ni Nanointerfaces, *ACS Energy Lett.*, 2018, **3**, 290–296.

90 Y. Wang, S. Pan, H. Li, D. Li, Y. Guo, S. Chi, C. Geng, S. Wu and Q. Yan, Facet-engineered photoelectrochemical nanocatalysts toward fast kinetic lithium-air batteries, *EES Catal.*, 2023, **1**, 312–321.

91 Q. Deng, Y. Yang, S. Qu, W. Wang, Y. Zhang, X. Ma, W. Yan and Y. Zhang, Electron structure and reaction pathway regulation on porous cobalt-doped CeO_2/graphene aerogel: A free-standing cathode for flexible and advanced Li-CO_2 batteries, *Energy Storage Mater.*, 2021, **42**, 484–492.
92 A. Mondal and A. Vomiero, 2D Transition Metal Dichalcogenides-Based Electrocatalysts for Hydrogen Evolution Reaction, *Adv. Funct. Mater.*, 2022, **32**, 2208994.
93 M. J. Theibault, C. Chandler, I. Dabo and H. D. Abruña, Transition Metal Dichalcogenides as Effective Catalysts for High-Rate Lithium-Sulfur Batteries, *ACS Catal.*, 2023, **13**, 3684–3691.
94 B. Lu, B. Chen, D. Wang, C. Li, R. Gao, Y. Liu, R. Mao, J. Yang and G. Zhou, Engineering the interfacial orientation of MoS_2/Co_9S_8 bidirectional catalysts with highly exposed active sites for reversible Li-CO_2 batteries, *Proc. Natl. Acad. Sci. U. S. A.*, 2023, **120**, e2216933120.
95 Z. Li, M. Li, X. Wang, D. Guan, W. Liu and J. Xu, In situ fabricated photo-electro-catalytic hybrid cathode for light-assisted lithium-CO_2 batteries, *J. Mater. Chem. A*, 2020, **8**, 14799–14806.
96 X. Xiao, H. Yu, H. Jin, M. Wu, Y. Fang, J. Sun, Z. Hu, T. Li, J. Wu, L. Huang, Y. Gogotsi and J. Zhou, Salt-Templated Synthesis of 2D Metallic MoN and Other Nitrides, *ACS Nano*, 2017, **11**, 2180–2186.
97 S. Wu, D. Deng, E. Zhang, H. Li and L. Xu, CoN nanoparticles anchored on ultra-thin N-doped graphene as the oxygen reduction electrocatalyst for highly stable zinc-air batteries, *Carbon*, 2022, **196**, 347–353.
98 Y. Fan, S. Ida, A. Staykov, T. Akbay, H. Hagiwara, J. Matsuda, K. Kaneko and T. Ishihara, Ni-Fe Nitride Nanoplates on Nitrogen-Doped Graphene as a Synergistic Catalyst for Reversible Oxygen Evolution Reaction and Rechargeable Zn-Air Battery, *Small*, 2017, **13**, 1700099.
99 Y. Lou, J. Liu, M. Liu and F. Wang, Hexagonal Fe_2N Coupled with N-Doped Carbon: Crystal-Plane-Dependent Electrocatalytic Activity for Oxygen Reduction, *ACS Catal.*, 2020, **10**, 2443–2451.
100 Y. Zhu, Q. Qian, Y. Chen, X. He, X. Shi, W. Wang, Z. Li, Y. Feng, G. Zhang and F. Cheng, Biphasic Transition Metal Nitride Electrode Promotes Nucleophile Oxidation Reaction for Practicable Hybrid Water Electrocatalysis, *Adv. Funct. Mater.*, 2023, **33**, 2300547.
101 S. Dutta, A. Indra, Y. Feng, H. Han and T. Song, Promoting electrocatalytic overall water splitting with nanohybrid of transition metal nitride-oxynitride, *Appl. Catal., B*, 2019, **241**, 521–527.
102 G. Qi, J. Zhang, L. Chen, B. Wang and J. Cheng, Binder-Free MoN Nanofibers Catalysts for Flexible 2-Electron Oxalate-Based Li-CO_2 Batteries with High Energy Efficiency, *Adv. Funct. Mater.*, 2022, **32**, 2112501.
103 Z. Cheng, Z. Wu, J. Chen, Y. Fang, S. Lin, J. Zhang, S. Xiang, Y. Zhou and Z. Zhang, Mo_2N-ZrO_2 Heterostructure Engineering in Freestanding Carbon Nanofibers for Upgrading Cycling Stability and Energy Efficiency of Li-CO_2 Batteries, *Small*, 2023, **19**, 2301685.
104 Y. Zhai, H. Tong, J. Deng, G. Li, Y. Hou, R. Zhang, J. Wang, Y. Lu, K. Liang, P. Chen, F. Dang and B. Kong, Super-assembled atomic Ir catalysts on Te substrates with synergistic catalytic capability for Li-CO_2 batteries, *Energy Storage Mater.*, 2021, **43**, 391–401.
105 K. Wang, D. Liu, L. Liu, X. Li, H. Wu, Z. Sun, M. Li, A. S. Vasenko, S. Ding, F. Wang and C. Xiao, Isolated Metalloid Tellurium Atomic Cluster on Nitrogen-Doped Carbon Nanosheet for High-Capacity Rechargeable Lithium-CO_2 Battery, *Adv. Sci.*, 2023, **10**, 2205959.
106 Y. Xu, H. Xue, X. Li, X. Fan, P. Li, T. Zhang, K. Chang, T. Wang and J. He, Application of metal-organic frameworks, covalent organic frameworks and their derivates for the metal-air batteries, *Nano Res. Energy*, 2023, **2**, e9120052.
107 T. Sun, J. Xie, W. Guo, D. Li and Q. Zhang, Covalent-Organic Frameworks: Advanced Organic Electrode Materials for Rechargeable Batteries, *Adv. Energy Mater.*, 2020, **10**, 1904199.
108 O. M. Yaghi, G. Li and H. Li, Selective binding and removal of guests in a microporous metal-organic framework, *Nature*, 1995, **378**, 703–706.
109 A. P. Côté, A. I. Benin, N. W. Ockwig, M. O'Keeffe, A. J. Matzger and O. M. Yaghi, Porous, Crystalline, Covalent Organic Frameworks, *Science*, 2005, **310**, 1166–1170.
110 D. Wang, T. Qiu, W. Guo, Z. Liang, H. Tabassum, D. Xia and R. Zou, Covalent organic framework-based materials for energy applications, *Energy Environ. Sci.*, 2021, **14**, 688–728.
111 A. Knebel and J. Caro, Metal-organic frameworks and covalent organic frameworks as disruptive membrane materials for energy-efficient gas separation, *Nat. Nanotechnol.*, 2022, **17**, 911–923.
112 S. Li, Y. Dong, J. Zhou, Y. Liu, J. Wang, X. Gao, Y. Han, P. Qi and B. Wang, Carbon dioxide in the cage: manganese metal-organic frameworks for high performance CO_2 electrodes in Li-CO_2 batteries, *Energy Environ. Sci.*, 2018, **11**, 1318–1325.
113 Y. Zhang, R. Zhong, M. Lu, J. Wang, C. Jiang, G. Gao, L. Dong, Y. Chen, S. Li and Y. Lan, Single Metal Site and Versatile Transfer Channel Merged into Covalent Organic Frameworks Facilitate High-Performance Li-CO_2 Batteries, *ACS Cent. Sci.*, 2021, **7**, 175–182.
114 S. Sung, D. Kumar, M. Gil-Sepulcre and M. Nippe, Electrocatalytic CO_2 Reduction by Imidazolium-Functionalized Molecular Catalysts, *J. Am. Chem. Soc.*, 2017, **139**, 13993–13996.
115 P. Wang, T. Li, Q. Wu, R. Du, Q. Zhang, W. Huang, C. Chen, Y. Fan, H. Chen, Y. Jia, S. Dai, Y. Qiu, K. Yan, Y. Meng, G. I. N. Waterhouse, L. Gu, Y. Zhao, W. Zhao and G. Chen, Molecular Assembled Electrocatalyst for Highly Selective CO_2 Fixation to C_{2+} Products, *ACS Nano*, 2022, **16**, 17021–17032.

116 Z. Zhang, W. Bai, Z. Cai, J. Cheng, H. Kuang, B. Dong, Y. Wang, K. Wang and J. Chen, Enhanced Electrochemical Performance of Aprotic Li-CO_2 Batteries with a Ruthenium-Complex-Based Mobile Catalyst, *Angew. Chem., Int. Ed.*, 2021, **60**, 16404–16408.

117 K. Seob Song, P. W. Fritz, D. F. Abbott, L. Nga Poon, C. M. Caridade, F. Gándara, V. Mougel and A. Coskun, Mixed-metal Ionothermal Synthesis of Metallophthalocyanine Covalent Organic Frameworks for CO_2 Capture and Conversion, *Angew. Chem., Int. Ed.*, 2023, **62**, e202309775.

118 E. Chen, M. Qiu, Y. Zhang, L. He, Y. Sun, H. Zheng, X. Wu, J. Zhang and Q. Lin, Energy Band Alignment and Redox-Active Sites in Metalloporphyrin-Spaced Metal-Catechol Frameworks for Enhanced CO_2 Photoreduction, *Angew. Chem., Int. Ed.*, 2022, **61**, e202111622.

119 H. Zheng, H. Li, Z. Zhang, X. Wang, Z. Jiang, Y. Tang, J. Zhang, B. Emley, Y. Zhang, H. Zhou, Y. Yao and Y. Liang, Dispersed Nickel Phthalocyanine Molecules on Carbon Nanotubes as Cathode Catalysts for Li-CO_2 Batteries, *Small*, 2023, **19**, 2302768.

120 Y. Wu, Z. Zhao and Z. Peng, Tailoring Li-CO_2 Electrochemistry Based on 4,4′-Bipyridine Redox Cycle, *ACS Energy Lett.*, 2023, **8**, 3430–3436.

121 Y. Wang, L. Song, L. Zheng, Y. Wang, J. Wu and J. Xu, Reversible Carbon Dioxide/Lithium Oxalate Regulation toward Advanced Aprotic Lithium Carbon Dioxide Battery, *Angew. Chem., Int. Ed.*, 2024, **63**, e202400132.

122 Y. Zhou and S. Guo, Recent advances in cathode catalyst architecture for lithium-oxygen batteries, *eScience*, 2023, **3**, 100123.